EUROPEAN ORGANIZATION FOR NUCLEAR RESEARCH (CERN)

CERN-EP-2025-058
2025/11/17

CMS-HIN-24-005

Jet fragmentation function and groomed substructure of bottom quark jets in proton-proton collisions at 5.02 TeV

The CMS Collaboration*

Abstract

A measurement of the substructure of bottom quark jets (b jets) in proton-proton (pp) collisions is presented. The measurement uses data collected in pp collisions at $\sqrt{s} = 5.02\,\text{TeV}$ recorded by the CMS experiment in 2017, corresponding to an integrated luminosity of $301\,\text{pb}^{-1}$. An algorithm to identify and cluster the charged decay daughters of b hadrons is developed for this analysis, which facilitates the exposure of the gluon radiation pattern of b jets using iterative Cambridge–Aachen declustering. The soft-drop-groomed jet radius, R_g, and momentum balance, z_g, of b quark jets are presented. These observables can be used to test perturbative quantum chromodynamics predictions that account for mass effects. Because the b hadron is partially reconstructed from its charged decay daughters, only charged particles are used for the jet substructure studies. In addition, a jet fragmentation function, $z_\text{b,ch}$, is measured, which is defined as the distribution of the ratio of the transverse momentum (p_T) of the partially reconstructed b hadron with respect to the charged-particle component of the jet p_T. The substructure variable distributions are unfolded to the charged-particle level. The b jet substructure is compared to the substructure of jets in an inclusive jet sample that is dominated by light-quark and gluon jets in order to assess the role of the b quark mass. A strong suppression of emissions at small R_g values is observed for b jets when compared to inclusive jets, consistent with the dead-cone effect. The measurement is also compared with theoretical predictions from Monte Carlo event generators. This is the first substructure measurement of b jets that clusters together the b hadron decay daughters.

Submitted to the Journal of High Energy Physics

*See Appendix B for the list of collaboration members

1 Introduction

Jets are the collimated showers of particles that result from the fragmentation of energetic quarks and gluons produced in high-energy particle collisions. They are one of the main objects used to improve our understanding of the strong nuclear force, which is described by quantum chromodynamics (QCD). Describing the formation of jets requires a detailed understanding of parton showering, i.e., the cascade of partons initiated by a highly energetic parton produced in the hard scattering, and the strongly coupled transition from partons into hadrons, known as hadronization. The radiation pattern of jets contains valuable information about their formation, which can be analyzed through jet substructure observables [1–3].

At a first approximation, the jet shower initiated by light-flavor quarks (up, down, or strange quarks) and gluons is governed by the infrared and collinear divergences of QCD and the running of the strong coupling, α_S. For heavy-flavor quark jets, i.e., those initiated by charm (c jets) or bottom quarks (b jets), there are no such divergences due to the heavy-quark masses, which effectively regularize them. In the quasi-collinear approximation, the Dokshitzer–Gribov–Lipatov–Altarelli–Parisi (DGLAP) splitting function for a gluon emission off a heavy quark ($Q \to Qg$) is given by

$$P_{Q\to Qg}(z) = \frac{1-z}{z} + \frac{z}{2} - 2\mu^2_{Qg}, \tag{1}$$

where z is the momentum fraction of the emission, and the mass ratio μ^2_{Qg} is given by

$$\mu^2_{Qg} = \frac{m^2_Q}{m^2_{Qg} - m^2_Q}, \tag{2}$$

where m_Q is the mass of the heavy quark and m_{Qg} is the invariant mass of the heavy-quark and gluon system [4–8]. Equation (1) has no soft divergence and it reduces to the standard DGLAP splitting function in the massless limit $m_Q \to 0$. As a consequence of the mass term, the momentum balance of a gluon emission off a heavy quark is expected to be more asymmetric in energy than it is for light quarks ($q \to qg$), or gluons ($g \to gg$), such that the heavy quark carries a larger amount of the momentum of the branching. This results in the heavy-flavor hadron that is observed experimentally carrying a substantial fraction of the heavy-quark momentum. The mass term also leads to the "dead-cone" effect, a general feature of quantum gauge field theories whereby collinear radiation is suppressed for massive particles. In QCD, the presence of a mass term in the quark propagator leads to a suppression of gluon emissions at a small angle relative to the recoiling heavy quark [9]. The probability to have a gluon emission with an opening angle θ with respect to the heavy quark in a $Q \to Qg$ branching is given by

$$d\mathcal{P}(\theta) \propto \frac{d\theta^2}{(\theta^2 + \theta_0^2)^2}, \tag{3}$$

where the parameter $\theta_0 = m_Q/E_Q$ dictates the effective size of the dead-cone angle, with E_Q being the energy of the heavy quark before the branching. The resulting dead-cone region is larger for more massive quarks or for a gluon emission from a less energetic heavy quark. In the massless limit, $\theta_0 \to 0$, one recovers the textbook collinear divergence of massless QCD. The dead-cone effect has been directly observed by the ALICE Collaboration using jets containing a fully reconstructed D^0 meson [10], but no comparable analysis has been performed yet for b jets. The effect is expected to be stronger for the latter.

Heavy-quark fragmentation is a rich, multiscale process. It is initiated by the highly energetic parton, carrying a transverse momentum (p_T) of the order of hundreds of GeV. It then evolves with the relative transverse momentum (k_T) of the $1 \to 2$ branchings in the parton shower, which ranges from a few GeV up to the order of the jet p_T. It also involves the mass of the heavy quark, which is about 1.5 and 4 GeV for charm and bottom quarks, respectively, and concludes with the energy scale associated with the transition from partons to hadrons, $\Lambda_{QCD} \approx 200$ MeV. The description of all of these effects in Monte Carlo (MC) event generators is not trivial. Thus, precision measurements that can constrain such aspects of heavy-flavor jet fragmentation can help shed light on them. In this analysis, the focus is on b jets, where mass effects are the strongest and for which CMS has developed tools for their identification ("tagging") [11]. Understanding the radiation pattern of b jets is also important to improve the description of top quark decays, as well as Higgs decays to bottom quark-antiquark pairs [1, 2, 12]. In addition, b jets are of interest for the characterization of the quark-gluon plasma properties in heavy ion collisions [13–16]. In this context, heavy-flavor jets introduce an additional energy scale in the multiscale process and can be used to effectively constrain the color factor of the jet shower. The dead-cone region has been identified as a phase space region where medium-induced radiation effects can be studied in a controlled environment [17, 18]. Previous measurements of the differential jet shape in proton-proton (pp) and Pb-Pb collisions [19] have indicated differences between the light-flavor jet population and b quark jet population, as well as their modifications due to medium effects, with hints of the dead-cone effect being at play.

Interpreting the data in terms of the underlying parton branching process becomes more challenging when b hadron decay daughters are treated on an equal footing with hadrons from b quark hadronization. This challenge arises, for example, in Lund-plane-based substructure observables or energy-energy correlators [17, 20], but it generally affects jet substructure observables. A recent reinterpretation of DELPHI and OPAL electron-positron (e^+e^-) data of light-hadron fragmentation functions measured in heavy-quark-enriched events [21, 22] showed that, after performing a simulation-based subtraction of the contribution of charm or bottom hadron decays, the resulting light-hadron fragmentation function is directly sensitive to the dead-cone effect [23]. Thus, a strategy to identify and isolate the decay daughters of heavy-flavor hadrons must be adopted in order to have a reliable interpretation of the data in terms of the underlying parton branching process. This approach is employed in this analysis and is discussed in more detail in Section 5.

In this analysis, we present a measurement of three jet substructure observables. Each of them probes different aspects of the fragmentation pattern of jets. Their technical definition is discussed in Section 4. The first two observables are the groomed jet radius, R_g, and momentum balance, z_g. They are obtained using the soft-drop (SD) grooming algorithm [24], which is a generalization of the modified mass-drop algorithm [25]. The SD algorithm allows for the decomposition of a full jet into a hard two-prong subjet structure, using iterative Cambridge–Aachen (CA) declustering [26]. The momentum balance z_g is the ratio of the transverse momentum carried by the softer subjet over the sum of the momenta of the two subjets, which is, to first approximation, related to the DGLAP splitting function. The groomed jet radius R_g is the angular opening between the softer and harder subjets. It is used as a proxy for the separation of the gluon emissions with respect to the b quark. Because of the dead-cone effect, small R_g emissions are expected to be suppressed. Recent theoretical calculations achieve next-to-leading logarithmic accuracy for the z_g and R_g distributions of heavy-flavor jets [27]. The third observable considered in the measurement is a jet fragmentation function, namely, the distribution of the fraction of the charged-particle transverse momentum of the jet carried by the charged-particle decay products of the b hadron, $z_{b,ch} = p_T^{b,ch} / p_T^{jet,ch}$. The fragmentation function for b hadrons was constrained at LEP [21, 22, 28], but recent CERN LHC measurements [29, 30] show that there are deviations with respect to predictions provided by MC event generators. These deviations suggest that there is a possible break of universality, likely resulting from the different color field environments of pp and e^+e^- collisions, which the present measurement can help clarify further. At leading order (LO) in perturbation theory, $z_{b,ch}$ and z_g should be strongly correlated, but such correlations are lost when accounting for higher-order and nonperturbative corrections [27]. Thus, $z_{b,ch}$ offers a complementary handle to the z_g observable. The jet substructure observables are measured both for inclusive jets and b jets and used to constrain the fragmentation of quark and gluon showers, providing important constraints to MC event generators and theoretical calculations.

The measurement is performed using data from pp collisions at $\sqrt{s} = 5.02\,\text{TeV}$ recorded by the CMS experiment in 2017. The CMS detector components, along with the reconstruction algorithms used, are described in Section 2. Details about the measured and simulated samples are presented in Section 3. The observable definitions and the strategy for the corrections are described in Sections 4 and 5, respectively. The systematic uncertainties associated with the corrected distributions are described in Section 6. The results are discussed in Section 7. A summary of the measurement is presented in Section 8. Tabulated results are provided in the HEPData record for this analysis [31].

2 The CMS detector and event reconstruction

The central feature of the CMS apparatus is a superconducting solenoid of 6 m internal diameter, providing a magnetic field of 3.8 T. Within the magnetic volume are a silicon pixel and strip tracker, a lead tungstate crystal electromagnetic calorimeter (ECAL), and a brass and scintillator hadron calorimeter (HCAL), each composed of a barrel and two endcap sections. Forward calorimeters extend the pseudorapidity (η) coverage provided by the barrel and endcap detectors. Muons are measured in gas-ionization detectors embedded in the steel flux-return yoke outside the solenoid. A more detailed description of the CMS detector, together with a definition of the coordinate system used and the relevant kinematic variables, is presented in Refs. [32, 33].

The primary vertex (PV) is taken to be the vertex corresponding to the hardest scattering in the event, evaluated using tracking information alone, as described in Section 9.4.1 of Ref. [34].

The particle-flow algorithm [35] aims to reconstruct and identify each individual particle in an event, with an optimized combination of information from the various elements of the CMS detector. The energy of photons is obtained from the ECAL measurement. The energy of electrons is determined from a combination of the electron momentum at the primary interaction vertex as determined by the tracker, the energy of the corresponding ECAL cluster, and the energy sum of all bremsstrahlung photons spatially compatible with originating from the electron track. The energy of muons is obtained from the curvature of the corresponding track. The energy of charged hadrons is determined from a combination of their momentum measured in the tracker and the matching ECAL and HCAL energy deposits, corrected for the response function of the calorimeters to hadronic showers. Finally, the energy of neutral hadrons, not associated with tracks, is obtained from the corrected ECAL and HCAL energies.

For each event, hadronic jets are clustered from these reconstructed particles using the anti-k_T algorithm [36] with $R = 0.4$, as implemented in FASTJET [37]. Jet momentum is determined as the vectorial sum of all particle momenta in the jet, and based on simulation, is found to be, on average, within 5 to 10% of the true momentum over the whole p_T spectrum and detector acceptance. Additional pp interactions within the same or nearby bunch crossings (pileup) can contribute additional tracks and calorimetric energy depositions, increasing the apparent jet momentum. To mitigate this effect, tracks identified to be originating from pileup vertices are discarded and an offset correction is applied to correct for remaining contributions [38]. Jet energy corrections are derived from simulation studies so that the average measured energy of jets becomes identical to that of particle-level jets. In situ measurements of the momentum balance in dijet, photon+jet, Z+jet, and multijet events are used to determine any residual differences between the jet energy scale in data and in simulation, and appropriate corrections are made [39]. The jet energy corrections used for this analysis were derived from a high-luminosity pp data sample at $\sqrt{s} = 13\,\text{TeV}$ collected also in 2017. We verify in the simulated samples used for this analysis that the corrected jet p_{T} agrees with the generated one in the kinematic range under study. Additional selection criteria are applied to each jet to remove jets potentially dominated by instrumental effects or reconstruction failures [38]. The jet energy resolution amounts typically to 10% at 100 GeV [39].

Jets containing one or more b hadrons are identified using PARTICLENET, a jet tagging tool based on the graph neural network architecture [40]. A selection on the PARTICLENET score is applied to select b jets with a 52% efficiency and 0.01% misidentification rate according to simulation.

Track reconstruction relies on the silicon tracker, which was upgraded at the start of 2017 with the installation of a new pixel detector [41]. The upgraded tracker measures particles up to $|\eta| = 3.0$ with typical resolutions of 1.5% in p_{T} and 20–75 μm in the transverse impact parameter [42] for nonisolated particles of $1 < p_{\mathrm{T}} < 10\,\text{GeV}$. Tracks used in this analysis are required to have $|\eta| < 2.4$ and $p_{\mathrm{T}} > 1\,\text{GeV}$. The η selection is chosen such that the b tagging performance is consistently high, aiming to reduce data-to-simulation differences in the clustering of the b hadron decay daughters. The $p_{\mathrm{T}} > 1\,\text{GeV}$ requirement is to avoid the fast drop of the track reconstruction efficiency at low p_{T}. To further discard tracks originating from pileup vertices, the absolute value of the longitudinal and transverse impact parameter of each track is required to be smaller than 17 and 0.2 cm, respectively [11].

Events of interest are selected using a two-tiered trigger system. The first level, composed of custom hardware processors, uses information from the calorimeters and muon detectors to select events at a rate of around 100 kHz within a fixed latency of about 4 μs [43]. The second level, known as the high-level trigger, consists of a farm of processors running a version of the full event reconstruction software optimized for fast processing, and reduces the event rate to around 1 kHz before data storage [44].

3 Data and simulated samples

This analysis uses pp collision data collected by the CMS experiment in 2017 at $\sqrt{s} = 5.02\,\text{TeV}$, corresponding to an integrated luminosity of $301 \pm 6\,\text{pb}^{-1}$ [45]. The average pileup activity during this run is approximately two interactions per bunch crossing. Events with high-p_{T} jets are collected with triggers requiring at least one jet with a p_{T} above 40, 60, 80, or 100 GeV. Because of the low pileup activity during the 5.02 TeV pp run, the 100 GeV trigger is able to sample the full luminosity. However, the lower threshold triggers only collected a part of the total luminosity, which affects the trigger efficiency. The latter is found to be about 99% for jets with an offline reconstructed p_{T} of 80 GeV, which is the lowest jet p_{T} value considered in this measurement. There are about two million jets satisfying the b tagging requirements described in Section 5 in the kinematic range considered.

Simulated events are used for the extraction of corrections and the estimation of systematic uncertainties on the measurement. The nominal simulated sample consists of QCD multijet events, generated at LO using PYTHIA8.240 [46], with the hadronization and underlying event parameters set to the CP5 tune [47]. The PYTHIA8 event generator implements a dipole parton shower ordered in p_{T}. The gluon radiation off of heavy quarks is taken into account via matrix element corrections [48, 49]. The quark and gluon hadronization is described by the Lund string model [50, 51], with the Bowler [52] modification of the fragmentation function for heavy quarks.

A second simulation sample is produced, also at LO, using HERWIG7.1.4 [53] with the CH3 tune [54]. In this case, the parton shower is governed by angular-ordered radiation [55], with mass-dependent splitting functions [55, 56]. The transition to hadrons is described by the cluster fragmentation model [57].

The generated samples use the next-to-next-to-LO NNPDF 3.1 [58] parton distribution functions with $\alpha_{\mathrm{S}}(m_{\mathrm{Z}}) = 0.118$, where m_{Z} represents the Z boson mass. Both generated samples are processed through a detailed simulation of the CMS detector with the GEANT4 toolkit [59]. Heavy-quark mass effects are modelled in the parton showers of PYTHIA8 CP5 and HERWIG7 CH3, allowing for an accurate description of soft gluon emission from heavy quarks over a wide angular region, including the collinear direction.

4 Observable definition

4.1 Groomed observables

Two of the substructure observables considered in this measurement are derived from the SD grooming algorithm [24]. This algorithm reclusters the original anti-k_{T} jet constituents using the CA algorithm [26], which is a pairwise clustering of particles (and subjets thereafter) that clusters the pair of subjets with the smallest rapidity-azimuth distance at each step of the clustering process. No explicit selection on the ΔR of the constituents with respect to the jet axis is applied for the reclustering step. This strong angular ordering of the CA algorithm intends to mimic the approximate angular ordering expected from color coherence effects in QCD showers [26, 60]. Once the CA clustering tree is constructed, the clustering history is followed in reverse, always following the hardest branch at each step of the declustering process, until the SD condition is satisfied:

$$\frac{\min(p_{\mathrm{T,1}}, p_{\mathrm{T,2}})}{p_{\mathrm{T,1}} + p_{\mathrm{T,2}}} > z_{\mathrm{cut}} \left(\frac{\Delta R_{1,2}}{R} \right)^{\beta}, \tag{4}$$

where $p_{\mathrm{T,i}}$ are the p_{T} of each subjet and $\Delta R_{1,2}$ is the distance on the rapidity-azimuth plane of the two subjets at each declustering step, i.e., $\Delta R_{1,2}^2 = \Delta y_{1,2}^2 + \Delta \phi_{1,2}^2$. The parameter R is the jet clustering distance parameter ($R = 0.4$ in this case), and z_{cut} and β are the SD grooming parameters, which are tunable. The softer subjet at each step of the declustering process may be considered as a proxy for a parton emission in the jet shower. When Eq. (4) is satisfied, the CA declustering iteration is stopped. The two resulting subjets are then used as proxies for the hard two-prong structure of the jet. The observables of interest are the groomed jet radius $R_{\mathrm{g}} = \Delta R_{1,2}$ and the groomed momentum balance $z_{\mathrm{g}} = p_{\mathrm{T,2}} / (p_{\mathrm{T,1}} + p_{\mathrm{T,2}})$, where $p_{\mathrm{T,2}}$ is the transverse momentum of the softer subjet. The groomed jet radius R_{g} is presented in the logarithmic form $\ln(R/R_{\mathrm{g}})$ in all the figures presented in this paper, following the standard representation for observables based on the CA clustering tree.

The grooming parameters z_{cut} and β determine the degree to which soft- and wide-angle radiation is being removed by the algorithm. Increasing the value of z_{cut} preferentially removes soft radiation, whereas decreasing values of β preferentially remove wide-angle radiation. We use the SD grooming parameters of $\beta = 0$ and $z_{\mathrm{cut}} = 0.1$. The value of $z_{\mathrm{cut}} = 0.1$ is the standard value used at the LHC, which represents a sufficiently low value to remove soft and wide-angle radiation. The choice of $\beta = 0$, together with $z_{\text{cut}} = 0.1$, facilitates the comparison with theoretical calculations of heavy-flavor quark substructure [27]. In addition, the suppression of emissions due to the dead-cone effect is clearest for $\beta = 0$, as illustrated in Fig. 3 of Ref. [27].

Jets that fail the SD condition are referred to as "one-pronged" or SD-untagged jets. The population of such jets is tracked in the analysis with an additional bin used for the unfolding corrections, as described later in the paper.

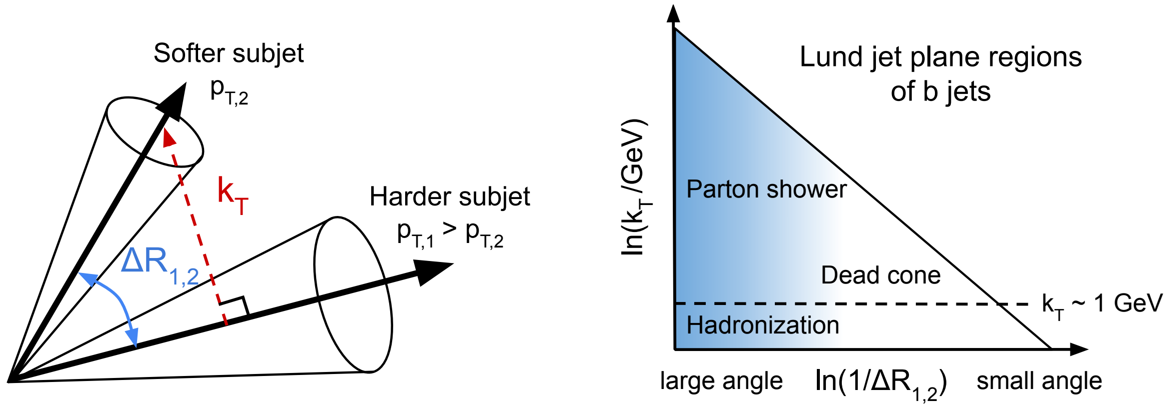

Figure 1: Left panel: A schematic diagram of two Cambridge–Aachen subjets, such as those found with the soft-drop grooming algorithm. The splitting angle $\Delta R_{1,2}$ and the relative transverse momentum k_{T} between the two subjets are annotated. Right panel: The Lund jet plane regions of bottom quark jets. The vertical axis is the logarithm of the relative transverse momentum $k_{\text{T}}/\,\text{GeV}$ of the softer subjet with respect to the harder subjet. The horizontal axis is the logarithm of the inverse of the opening angle between the softer and harder subjets, $\Delta R_{1,2}$. The Lund jet plane is expected to be dominated by hadronization effects for k_{T} below the GeV scale. Above the GeV scale, the Lund jet plane provides information on the parton showering description. Emissions are suppressed at small angles due to the dead-cone effect. The b hadron decays (not depicted) populate the same region. The blue shading, fading from left to right, represents the density of emissions in the primary Lund jet plane for b quark jets.

The relative transverse momentum of the softer subjet with respect to the harder subjet $k_{\text{T}} = p_{\text{T},2} R_{\text{g}}$, which is a measure of the energy scale of the branching, is used as an additional selection requirement on the SD emissions considered in the analysis. We select SD-groomed emissions that satisfy $k_{\text{T}} > 1\,\text{GeV}$, which is a minimal momentum scale where hadronization effects are less strong [17, 61]. As pointed out in Ref. [17], such a selection requirement improves the hadron-to-parton correspondence of the substructure of jets and enhances the visibility of the dead-cone effect at small R_{g} values. The jets that satisfy the SD condition, but where the emission has $k_{\text{T}} < 1\,\text{GeV}$, are grouped together with the population of jets that do not satisfy the SD grooming criteria.

In PYTHIA8 CP5, around 3% of inclusive jets fail the SD grooming criteria, while approximately 37% of inclusive jets satisfy the SD condition but with $k_{\text{T}} < 1\,\text{GeV}$. For b jets, these fractions are substantially different, 46% and 25%, respectively, due to the suppressed collinear radiation and hard fragmentation of the b quark.

Groomed jet observables [62–67], as well as other observables based on the CA clustering tree [68–70], have been measured before for inclusive jet collections. In the case of charm quark jets, jets containing a D^0 meson have been used for substructure measurements by the ALICE Collaboration [10, 71]. However, the approach based on exclusive decays is much more limiting in the case of b hadrons, since the fraction of b hadrons that decay exclusively into charged particles is of the order of 0.1% [72]. As a result, different LHC measurements of b jet substructure so far [73, 74] have not taken into account the effect of the decay of b hadrons, i.e., the decay daughters are treated equally with the hadrons that are produced from the transition from partons to hadrons in the hadronization process. It is therefore challenging to disentangle mass effects, such as the presence of the dead cone, or to separate the parton cascade from the strong interactions from the b hadron decays, which are primarily associated with weak-interaction decays.

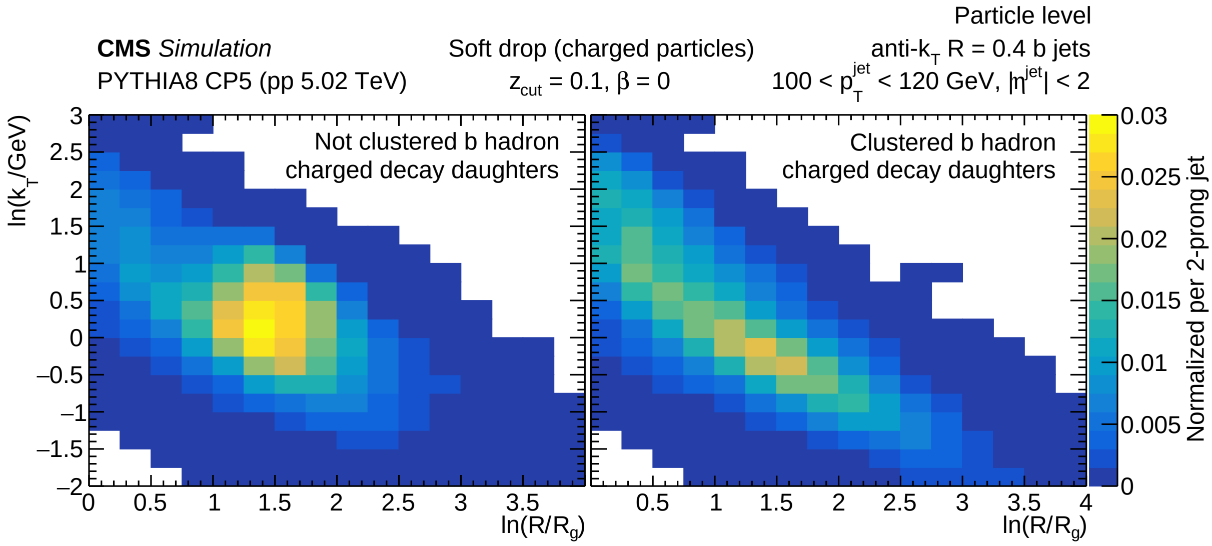

Figure 2: The Lund jet plane of the soft-drop emissions of b quark jets at the particle-level of the PYTHIA8 CP5 simulation. The vertical axis is the logarithm of the k_T/ GeV of the emission, whereas the horizontal axis is the logarithm of R/R_g, such that large-angle emissions populate the left-hand side of the diagrams and small-angle emissions populate the right-hand side. On the left-hand side, the SD algorithm is applied to the charged-particle jet constituents including the b hadron decay daughters. On the right-hand side, the b hadron charged decay daughters have been clustered together prior to the SD grooming, i.e., the charged component of the b hadron remains intact. The effect of the decays can be observed in the yellow hotspot at small angles and low k_T on the left.

To visualize the effect of the b hadron decays, it is instructive to use a representation of the substructure of the jet that accounts for momentum and angular information where different jet showering effects can be separated. This can be done, for example, via the Lund jet plane [61], which is a two-dimensional representation of the phase space of intrajet $1 \to 2$ emissions constructed using the CA clustering tree. The vertical axis of this plane corresponds to the logarithm of k_T/ GeV and the horizontal axis is the logarithm of the inverse of the opening angle $\Delta R_{1,2}$. The Lund jet plane allows for the identification of regions that are dominated by the short-distance physics (parton shower) and long-distance physics (hadronization) depending on the k_T region of interest. The Lund jet plane enables the separation of different effects in a modular fashion, such that at low k_T (approximately below 1GeV) it is dominated by hadronization effects, at large angles it is dominated by the parton showering description, and at small angles one can isolate the suppression of emissions expected from the dead-cone effect. In Fig. 1 (left) we give a schematic representation of two subjets, annotating the splitting angle and relative transverse momentum between them, while in Fig. 1 (right) we observe the different regions of the b jet showers at the hadron level, assuming that there are no b hadron decays.

By analyzing the kinematics of the SD emissions in simulation in terms of the Lund jet plane, as in Fig. 2, we observe that the effect of the b hadron decays on the substructure observable distributions is significant. The Lund jet plane of SD emissions of b jets is highly influenced by the presence of decay products (left-hand-side distribution of Fig. 2) or by their absence (right-hand-side distribution of Fig. 2). Left untreated, the b hadron decays degrade the correspondence between the jet substructure variables and the underlying QCD splitting processes. It is therefore necessary to address the heavy-flavor hadron decays in order to make any meaningful conclusions about the hard substructure of heavy-flavor jets.

4.2 Partial b hadron reconstruction

In this analysis, to mitigate the distortions caused by the b quark decay daughters, an algorithm that reconstructs the b hadron from its charged decay products is developed. This algorithm treats inclusively all possible decay channels of the b hadron. A multivariate analysis is performed to identify charged particles originating from the b hadron decay using events generated by PYTHIA8 CP5. Once all charged particles in the jet have been classified, the assumed decay product four-momenta are summed vectorially and such decay product particles are replaced by the partially reconstructed b hadron four-momentum. The CA reclustering and declustering process is then applied on the new set of jet constituents, which no longer includes the decay products.

The model used in the analysis is a gradient boosted decision tree. The input variables are characteristics of the charged particle, such as its reconstructed track and associated secondary vertex information. The charged particles used in the training and validation of the model have $p_{\mathrm{T}}^{\mathrm{track}} > 1\,\mathrm{GeV}$ and come from b-tagged jets with $p_{\mathrm{T}}^{\mathrm{jet}} > 30\,\mathrm{GeV}$. All reconstructed particles considered are matched to generated particles, so that they either come from the primary vertex (background) or the b hadron decay (signal). The working point selected corresponds to 92% signal efficiency and 95% background rejection rate according to simulation. The performance of the classifier can also be showcased in the simulated detector-level distributions of the groomed observables R_{g} and z_{g}, as presented in the left and right panels of Fig. 3, respectively. The distributions including the partially reconstructed b hadron (orange dashed-dotted curve) approach the particle-level distribution (blue solid curve) significantly more than in the case where the b hadron decay daughters are not clustered (violet dotted curve).

With the algorithm described in this section, the b hadron can be partially reconstructed using charged particles. Thus, using neutral particles in addition to the charged ones for the jet substructure observables can lead to b hadron neutral decay daughters populating the small angle region of the Lund jet plane. This would make the interpretation of the substructure in terms of QCD cascades more challenging, which is the issue addressed via the partial b hadron reconstruction. Therefore, the jet substructure observables are also computed using only charged-particle tracks. Using only the charged particles has the additional advantage of yielding better angular and momentum resolution. A $p_{\mathrm{T}}^{\mathrm{track}} > 1\,\mathrm{GeV}$ selection is applied in the CA reclustering step, in order to avoid the fast decrease in track reconstruction efficiency and minimize possible data-to-simulation differences. Although the charged-particle jet substructure is not collinear safe, comparisons to theoretical predictions of certain observables may still be possible by making additional nonperturbative corrections to account for the use of only the charged component of the jet. The charged-particle jet substructure variable distributions can be used for MC event generator tuning of the QCD cascade of b jets.

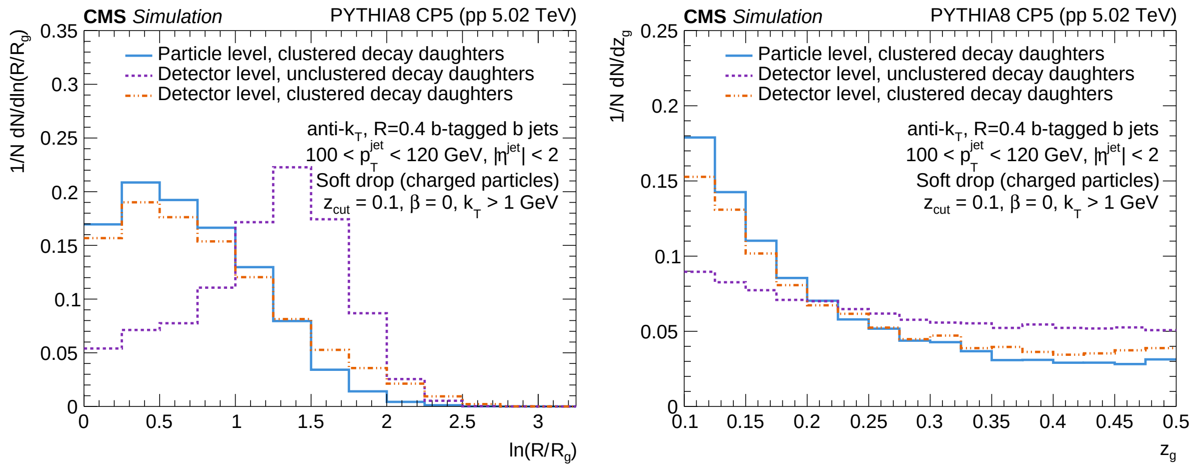

Figure 3: The modification of the R_g (left) and z_g (right) distributions at the detector level without (violet dotted curve) and with (orange dashed-dotted curve) the partial reconstruction of the b hadron, compared to the particle-level distribution with the charged part of the generated b hadron intact (blue solid curve). The events are produced by the PYTHIA8 CP5 generator.

4.3 The jet fragmentation function

With a partially clustered b hadron, it is possible to study other aspects of b jet fragmentation, such as the fraction of the jet transverse momentum carried by the b hadron. Since the b hadron is clustered using only charged particles, we compare its p_T to the p_T of the charged-particle components of the jet,

$$z_{b,ch} = \frac{p_T^{b,ch}}{p_T^{jet,ch}}, \tag{5}$$

where $p_T^{b,ch}$ is the p_T of the partially reconstructed b hadron and $p_T^{jet,ch}$ is the p_T of the charged-particle component of the jet. We refer to Eq. (5) as the b jet fragmentation function. The $k_T > 1\,\text{GeV}$ selection that is used for the groomed jet substructure observables is not used for $z_{b,ch}$, so $z_{b,ch}$ includes information complementary to the one contained in R_g and z_g. There are existing measurements of the fragmentation function of b hadrons using exclusive decays, e.g., $B^\pm \to J/\psi K^\pm$, in jets [29, 75]. The ATLAS Collaboration has followed a cut-based approach to cluster the b hadron decay daughters for b jets produced in top quark pair production [30]. In that measurement, the four-momentum of the reconstructed secondary vertex in the event is treated as a proxy for the b hadron in order to measure its fragmentation function and related properties. In the approach presented in this paper, we optimize the partial reconstruction of b hadron candidates using all jet charged-particle constituents and the secondary vertices they are associated with as input to a multivariate analysis. Charged particles not associated with a secondary vertex are also considered.

5 Analysis method and corrections

5.1 The b tagging efficiency scale factors

A subset of b jets is selected from the inclusive jet sample, using the PARTICLENET tagger [40]. The resulting signal efficiency in simulation may differ from the one found in data depending on the jet properties. In this analysis, we only measure per-jet normalized quantities, which are insensitive to an overall data-to-simulation difference in tagging performance. However, data-to-simulation differences as functions of the observables are potential sources of systematic uncertainty. To account for such effects, we evaluate scale factors for the b tagging performance difference of PARTICLENET between data and simulation, using the "reference lifetime algorithm" described in Ref. [76]. The scale factors are applied as a bin-by-bin correction on the detector-level distributions of b jets, in order to mimic the b tagging performance in the MC simulation used in the unfolding procedure.

5.2 Residual background subtraction

The set of b-tagged jets in the considered kinematic range consists of 83% jets with exactly one b hadron (single-b jets), 16% jets with two or more b hadrons (double-b jets) and 1% jets coming from gluons, and light and c quarks (light+c jets), according to the simulated sample from PYTHIA8 CP5. The main residual background contamination coming from double-b jets, resulting for example from gluon splitting processes, is detrimental to the measurement, as the two or more b hadrons are merged into one during the partial reconstruction process. This effect is minimized by fitting the partially reconstructed b hadron mass distribution to templates coming from simulation. The template fit is performed in bins of the measured observables.

We use three templates: one for single-b jets, one for double-b jets, and one light+c jets. Because of the high b jet purity of the selected b tagging working point, the light+c background is strongly suppressed and the corresponding template is poorly populated. It is therefore combined with the single-b template, fixing the light+c over single-b fraction to the value obtained from the PYTHIA8 CP5 simulation. We assign an uncertainty associated with this template combination step, as described in Section 6. Additionally, we assign an uncertainty associated with the template shape by using HERWIG7 CH3 as an alternative MC generator, which is also discussed in Section 6. Examples of the template fit performed in one bin of each observable are given in Fig. 4. The detector-level yield distributions, with the aforementioned b tagging efficiency scale factors applied, are multiplied by the extracted single-b jet fractions determined from the template fitting procedure.

5.3 Unfolding

Bin-to-bin migration effects are corrected for using two-dimensional unregularized unfolding with the ROOUNFOLD package [77, 78], in bins of jet p_{T} and the observable of interest. The jet p_{T} includes three bins, where the middle bin is the one reported in the measurement, and the bins below and above account for the bulk of the migrations. The fragmentation function $z_{\mathrm{b,ch}}$ spans the whole range from 0 to 1, where the edges are included in the first and last bins, respectively. Regarding the groomed observables, the jets that fail the SD condition or have $k_{\mathrm{T}} < 1\,\mathrm{GeV}$ are included in a dedicated bin, such that they can migrate from SD-untagged to SD-tagged from the particle to the detector level or vice versa. In the case of R_{g}, an overflow bin of large $\ln(R/R_{\mathrm{g}})$ (small R_{g}) is also included. This ensures that all possible migrations are taken into account, and the same collection of jets is considered for all three observables. Both the detector and particle levels correspond to the charged-particle substructure and use the same binning.

The fraction of reconstructed jets without a generated jet counterpart is found to be negligible. A reconstruction purity bin-by-bin correction is applied, to account for reconstructed jets which were generated with a p_{T} outside the kinematic range. In the reported jet p_{T} range of 100 to 120 GeV, this corresponds to 3–7% of reconstructed jets in the PYTHIA8 CP5 samples. The resulting distributions are then unfolded to the charged-particle level using unregularized matrix inversion. The fraction of jets migrating to neighboring bins is about 50%. The charged-

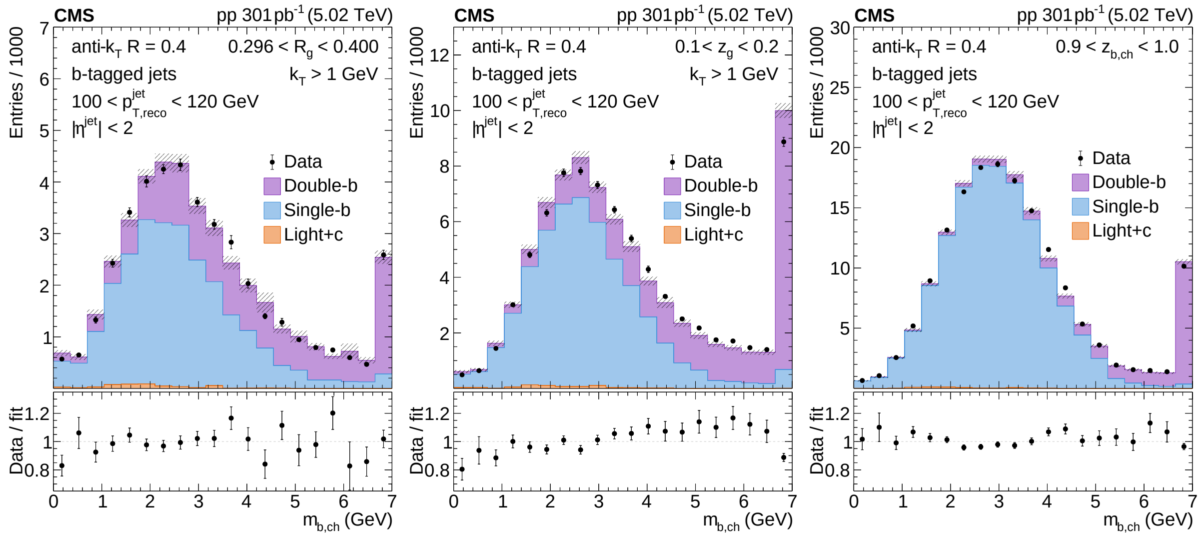

Figure 4: Examples of the fit of the partially reconstructed b hadron mass to double-b, single-b, and light+c jet templates coming from PYTHIA8 CP5. From left to right, the distributions in selected R_g, z_g, and $z_{b,ch}$ bins are presented. The black points represent the data counts, while the violet, blue, and orange filled curves represent the double-b, single-b, and light+c jet templates, with the fractions acquired from the fit. The ratio between the data and the fit values is presented in the lower panels.

particle-level result is corrected for the reconstruction efficiency, which accounts for generated jets that were reconstructed outside the jet p_T range. This corresponds to a 3–6% correction in each bin.

5.4 The b tagging efficiency correction

The charged-particle-level result is corrected for biases that are introduced as a result of the use of b tagging. All b tagging algorithms are prone to selecting b jets with specific qualities which make them easier to identify, such as high-multiplicity decay vertices. To account for this bias, we calculate a b tagging efficiency correction at the particle level of the simulation. This correction corresponds to the inverse of the b jet efficiency in each bin and is applied as a multiplicative per-bin factor, as a function of the jet substructure observable.

A sample of inclusive jets is used as a reference for the substructure variables. These serve as a proxy for a sample of jets where mass effects are absent, due to the dominance of light-quark and gluon jets in inclusive jets. The inclusive jet distributions are also unfolded to the stable-particle level.

6 Systematic uncertainties

Systematic uncertainties originating from several theoretical and experimental sources are considered in this study. The individual variations are propagated through the relevant steps in the analysis and the fully corrected result is compared to the nominal one. All relative uncertainties resulting from a single variation, such as the shower and hadronization model, are symmetrized around zero. In two-point variations, i.e., varying a parameter up and down within its uncertainty, such as the jet energy resolution, the larger of the two resulting uncertainties is chosen and symmetrized in each bin. The following systematic uncertainties apply both to inclusive and b jets and are propagated through the corrections to the stable-particle level.

Shower and hadronization modeling uncertainty: This uncertainty is estimated by building the response matrix, along with the reconstruction purity and efficiency corrections, using events simulated by the HERWIG7 CH3 generator instead of the nominal PYTHIA8 CP5. Since HERWIG7 CH3 has a different parton shower algorithm and a different hadronization model, this uncertainty mostly quantifies the difference in the detector response at the full-jet and the subjet levels.

Parton shower scale uncertainties: To estimate the theoretical uncertainty due to missing higher-order corrections in the perturbative calculation of the parton shower of PYTHIA8 CP5, we consider variations of the renormalization scale for the final-state radiation (FSR) and initial-state radiation (ISR) by factors of 2 and 1/2, corresponding to up and down variations, independently for the two sources [79, 80]. In practice, the nominal PYTHIA8 CP5 generated sample is reweighted at the particle level as a function of the jet p_{T} and of the substructure variable of interest in order to reproduce the distribution resulting from the FSR and ISR variations. The unfolding is repeated for each of these variations. Generally, these up and down variations have symmetric effects on the jet substructure variable distributions and in the associated systematic uncertainties. The effect of the variations of the ISR renormalization scale are smaller than the ones from FSR. The resulting uncertainties are symmetrized per source (FSR, ISR) and added in quadrature.

Tracking efficiency uncertainty: Track reconstruction in high-density environments, such as the core of a jet, is prone to mismodeling in simulation. To account for that, we propagate a tracking reconstruction efficiency uncertainty through the unfolding procedure. This is done by randomly removing 3% of the reconstructed tracks in simulation during the substructure extraction. This value covers the residual differences observed in data and simulation for tracking in the jet core in the context of jet energy scale determination [39].

Response matrix statistical uncertainties: We assign a systematic uncertainty to the measurement due to the finite number of simulated events that populate the response matrix by employing the "jackknife" resampling technique [81–83], as used previously in Ref. [65]. In this method, we create ten samples, each with 90% of the simulated events, so that each event is excluded exactly once in the resampling procedure. We then obtain ten different fully corrected distributions, using each of these samples in the unfolding. The standard deviation of this ensemble of distributions, scaled by 10/9 to account for using 90% of the full sample for each subset of events, is taken as the statistical uncertainty from the limited sample size of the MC simulation.

Jet energy scale and resolution uncertainties: The jet energy scale uncertainty is estimated by varying the detector-level jet p_{T} in simulation within the η-p_{T} dependent jet energy scale uncertainty [39]. It is decomposed into multiple sources, and the unfolding is repeated for each subcomponent. The dominant uncertainty for the inclusive jets comes from the flavor component, as a result of the mixture of quark and gluon jets, while it is smaller for the b jets. The per-source symmetrized uncertainties are added in quadrature. The jet energy resolution uncertainty is also considered. As described in Section 2, jet energy resolution scale factors are already applied to the detector-level jet p_{T} in simulation in order to account for differences between simulation and data. An uncertainty in the measurement is derived by varying the aforementioned scale factors within their uncertainties.

There are also uncertainties considered that only apply to b jets. These uncertainties relate to the b tagging and background subtraction procedures and are applied to the corresponding steps of the analysis.

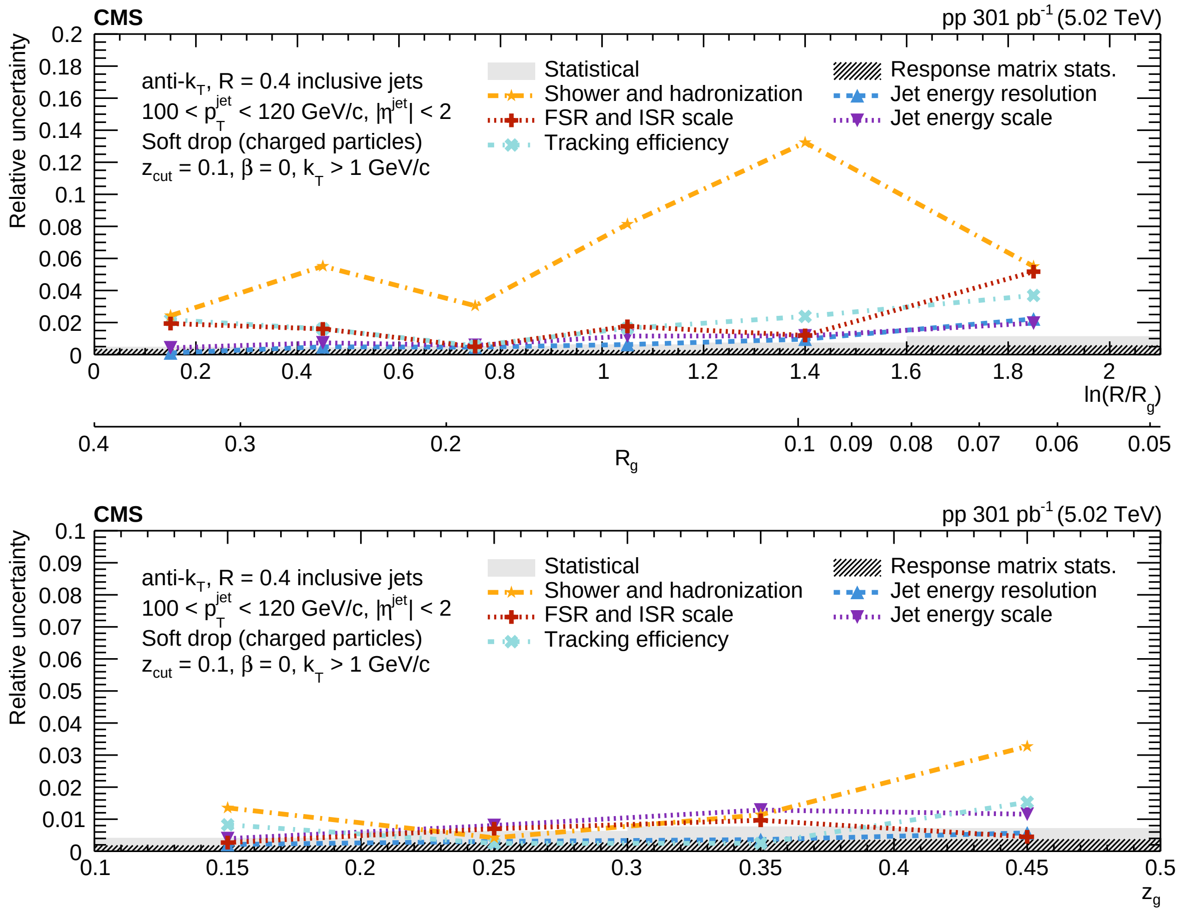

Figure 5: The breakdown of systematic uncertainties for inclusive jets (upper panel: R_g, lower panel: z_g). The statistical uncertainty is also shown in gray shaded boxes.

b tagging efficiency uncertainty: As described in Section 5, an efficiency correction is applied to account for the bias introduced by the use of b tagging. This correction is calculated from the PYTHIA8 CP5 simulation. To account for differences in the b tagging performance between the simulation and the data, scale factors are applied to the data prior to the unfolding. We assign an uncertainty in the b tagging efficiency by varying the scale factors within their uncertainty.

Residual background subtraction uncertainties: We consider two sources of systematic uncertainty related to the method used for the subtraction of the residual gluon, light-quark, and c quark jet components, as well as jets including more than one b quark, from the b-tagged jet collection. In one case, we replace the nominal templates based on PYTHIA8 CP5 simulated events with the ones derived from the HERWIG7 CH3 generator, which affects the template shapes. In the other case, we vary the MC fraction of light+c relative to the single-b jets in the simulation. This corresponds to an up and down variation of the fraction by 100% before the two templates are combined, as described in Section 5. In both cases, a new single-b jet fraction is extracted and propagated. We then compare these variations with the nominal distributions and extract the b jet fraction and light+c misidentification rate uncertainties, respectively. Each of these pieces is considered to be independent from each other.

The size of the systematic uncertainties is presented in Fig. 5 for inclusive jets and Fig. 6 for single-b jets. The leading uncertainties for both samples of jets are related to the physics model,

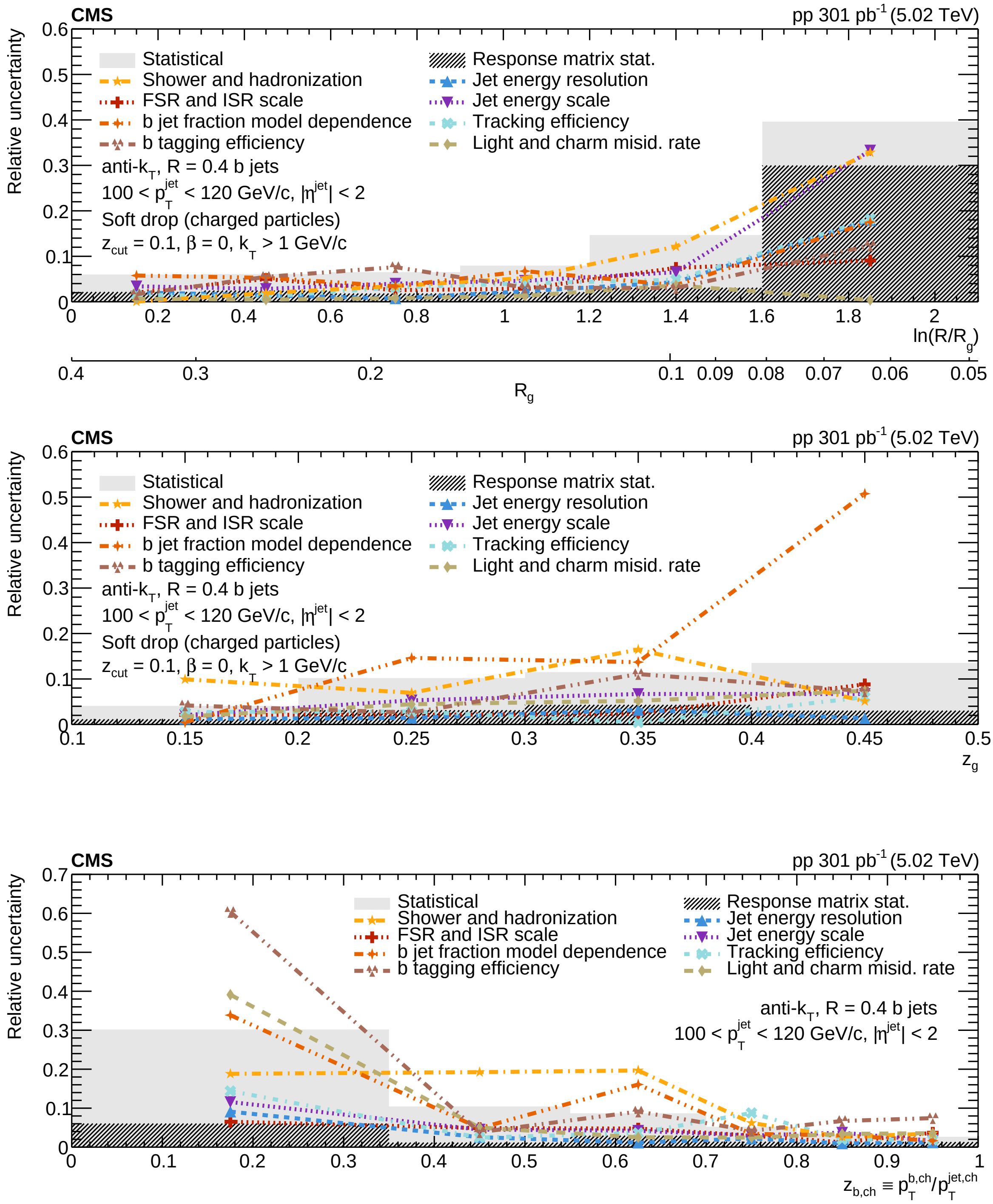

Figure 6: The breakdown of systematic uncertainties for b jets (upper panel: R_g, middle panel: z_g, lower panel: $z_{b,ch}$). The statistical uncertainty is also shown in gray shaded boxes.

which affects the detector response at the substructure and full jet levels. Namely, the shower and hadronization model, the parton shower scale and the model dependence of the b jet fraction are dominant, reaching up to 14% uncertainty for inclusive jets and 20% for b jets, with the exception of the smallest R_g (largest $\ln(R/R_g)$) bin. An improved description of the MC generators could improve these uncertainties in the future. In the case of b jets, we also observe the b tagging efficiency uncertainty become important, especially in the small $z_{b,ch}$ region.

7 Results

The fully corrected distributions of R_g and z_g for inclusive jets and b jets are presented in Figs. 7 and 8, respectively. The fraction of jets that do not satisfy the SD grooming condition or have $k_T < 1$ GeV is found to be 38.5 ± 0.1 (stat) $\pm$ 2.3 (syst)% for inclusive jets, whereas PYTHIA8 CP5 (HERWIG7 CH3) predicts 40.7% (36.3%). For b jets, the fraction is found to be 66.2 ± 0.9 (stat) $\pm$ 2.7 (syst)% in the data and 71.0% (62.3%) in PYTHIA8 CP5 (HERWIG7 CH3).

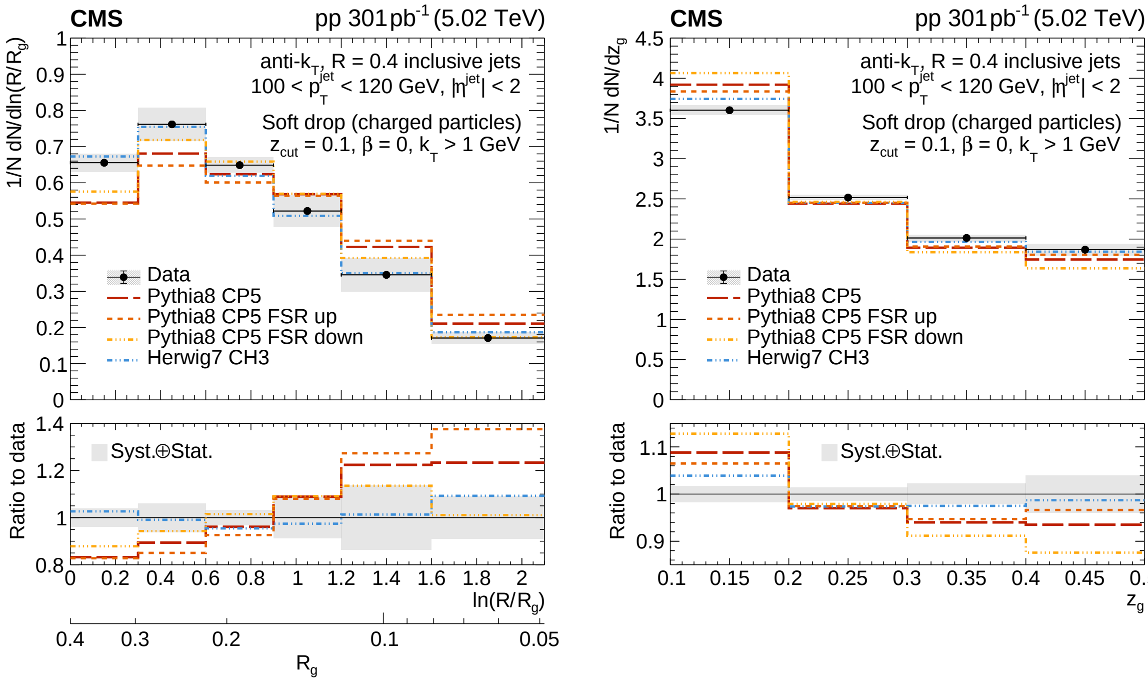

Figure 7: Distributions of groomed substructure observables R_g (left) and z_g (right) corrected to the charged-particle level for inclusive jets. The gray band represents the systematic uncertainties added in quadrature, while the vertical bars represent the statistical uncertainty. Distributions coming from the PYTHIA8 CP5 and HERWIG7 CH3 MC event generators are also presented. The ratio of the MC simulations to the data is presented in the lower panels.

Strong deviations are observed from the PYTHIA8 CP5 distributions for inclusive jets. More specifically, the PYTHIA8 CP5 R_g distribution is shifted to larger $\ln(R/R_g)$ (smaller R_g) values with respect to the data. The PYTHIA8 CP5 prediction also slightly overestimates the number of jets with a small momentum balance z_g between the two subjets. On the other hand, HERWIG7 CH3 has a good agreement with the data in both observables.

In the case of b jets, deviations are also observed for R_g, while the two generators agree with the data within the experimental uncertainties for z_g. The agreement of HERWIG7 CH3 with the measured R_g distribution is less good for b jets than for inclusive jets, suggesting that there might be mismodeling as a result of the presence of mass effects.

The jet fragmentation function $z_{b,ch}$, i.e., the charged-particle momentum fraction of the partially reconstructed b hadron with respect to the jet, and its comparison with the simulated predictions, is presented in Fig. 9. The distribution peaks at high $z_{b,ch}$, indicating that the b hadron holds most of the momentum during the fragmentation process. The PYTHIA8 CP5

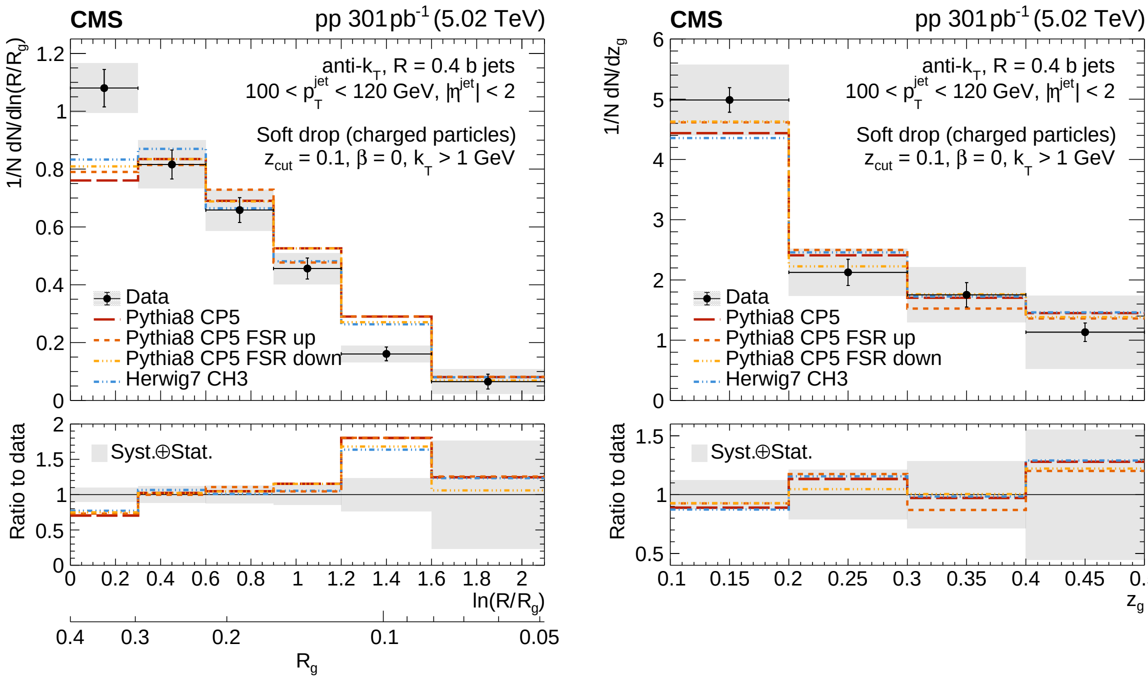

Figure 8: Distributions of the groomed substructure observables R_g (left) and z_g (right) corrected to the charged-particle level for b jets. Distributions coming from the PYTHIA8 CP5 and HERWIG7 CH3 MC event generators are also presented. The ratio of the MC simulations to the data is presented in the lower panels.

prediction agrees with the data within the experimental uncertainty, while the HERWIG7 distribution has a slightly larger width.

Finally, we present the comparison between inclusive jets and b jets for the groomed observables in Fig. 10 and comparisons with the predictions in Fig. 11. Each source of systematic uncertainty is propagated as correlated in the ratio, assuming they are fully correlated bin-by-bin. This is with the exception of the response matrix statistical uncertainties, b tagging uncertainties, as well as the uncertainties associated with the background subtraction, which are assumed to be fully uncorrelated. In the case of the jet energy scale uncertainties, the flavor-related components are decorrelated for the b jet to inclusive jet ratio. The inclusive jet sample is dominated by light-quark and gluon jets, so it serves as a proxy of the substructure of jets in the massless limit.

In the case of R_g, we observe a strong suppression of emissions at small R_g (large $\ln(R/R_g)$) values in b jets with respect to the inclusive jet reference. The suppression increases monotonically with decreasing R_g (increasing $\ln(R/R_g)$). This is qualitatively consistent with the dead-cone effect expectations. The PYTHIA8 CP5 predictions, while they do not describe well the R_g distributions of b jets and inclusive jets separately, they reproduce the b-to-inclusive jet ratio better. This suggests that the jet shower is mismodeled in a similar way for b jets and inclusive jets, whereas the small-angle emission suppression due to mass effects is modeled well. On the other hand, HERWIG7 CH3 captures less well the shape of the R_g ratio.

The b jets also tend to favor the smaller momentum balance z_g region more than the inclusive jets. This indicates that the b quarks take up a larger fraction of the splitting momentum when emitting gluons than other partons, consistent with the qualitative expectation from the DGLAP massive parton splitting function. Both generators agree with the data in the z_g ratio,

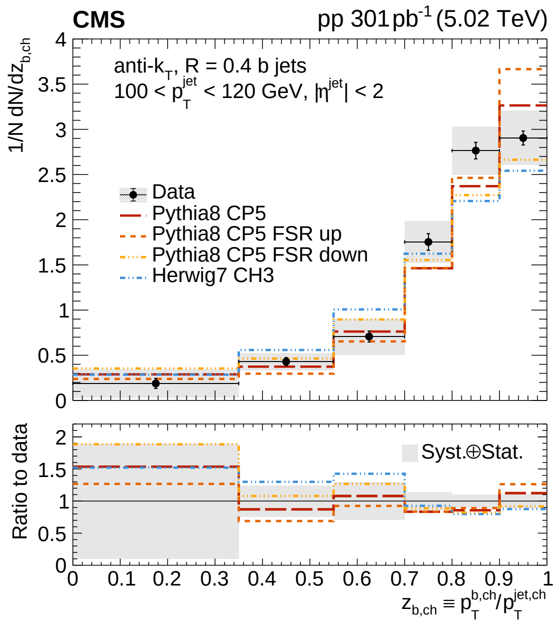

Figure 9: The distribution of the jet fragmentation function $z_{\mathrm{b,ch}}$ corrected to the charged-particle level. Distributions coming from the PYTHIA8 CP5 and HERWIG7 CH3 MC event generators are also presented. The ratio of the MC simulations to the data is presented in the lower panel.

within the experimental uncertainties.

In this study, the inclusive jet sample is a mixture of quark- and gluon-initiated jets. Thus, to illustrate the effect of the heavy-quark mass, it is instructive to compare the ratio of b jet to light-quark jet distributions in PYTHIA8 CP5 simulated events, which describe the data well in the b jet over inclusive jet case. Figure 12 (left) shows that the suppression of collinear emissions in b jets with respect to light-quark jets is stronger than the one of the ratio of b jets to inclusive jets. This is because gluons, which dominate the inclusive jet sample, have on average broader patterns than light-quark jets. The momentum balance z_{g}, as shown in Fig. 12 (right), is more asymmetric in b jets with respect to the light-quark jets according to the simulation.

8 Summary

This paper presents measurements of the substructure of bottom quark jets (b jets) and of inclusive jets in proton-proton collisions at $\sqrt{s} = 5.02\,\mathrm{TeV}$ using data corresponding to an integrated luminosity of $301\,\mathrm{pb}^{-1}$ collected in 2017 with the CMS experiment. The jets considered were initially clustered with the anti-k_{T} algorithm using a distance parameter of $R = 0.4$, and had transverse momentum $100 < p_{\mathrm{T}} < 120\,\mathrm{GeV}$ and pseudorapidity $|\eta| < 2$. The substructure observables are calculated using the charged-particle constituents of the jets. The groomed jet radius R_{g}, groomed momentum balance z_{g}, and the jet fragmentation function $z_{\mathrm{b,ch}}$ are measured and corrected to the charged-particle level. Corrections include background subtraction, migration effects, and efficiency corrections.

A challenge in the interpretation of previous b jet substructure measurements is that the b hadron decay daughters are clustered in the jet on an equal footing with the hadrons that are produced from the transition from partons to hadrons. To better understand the gluon ra-

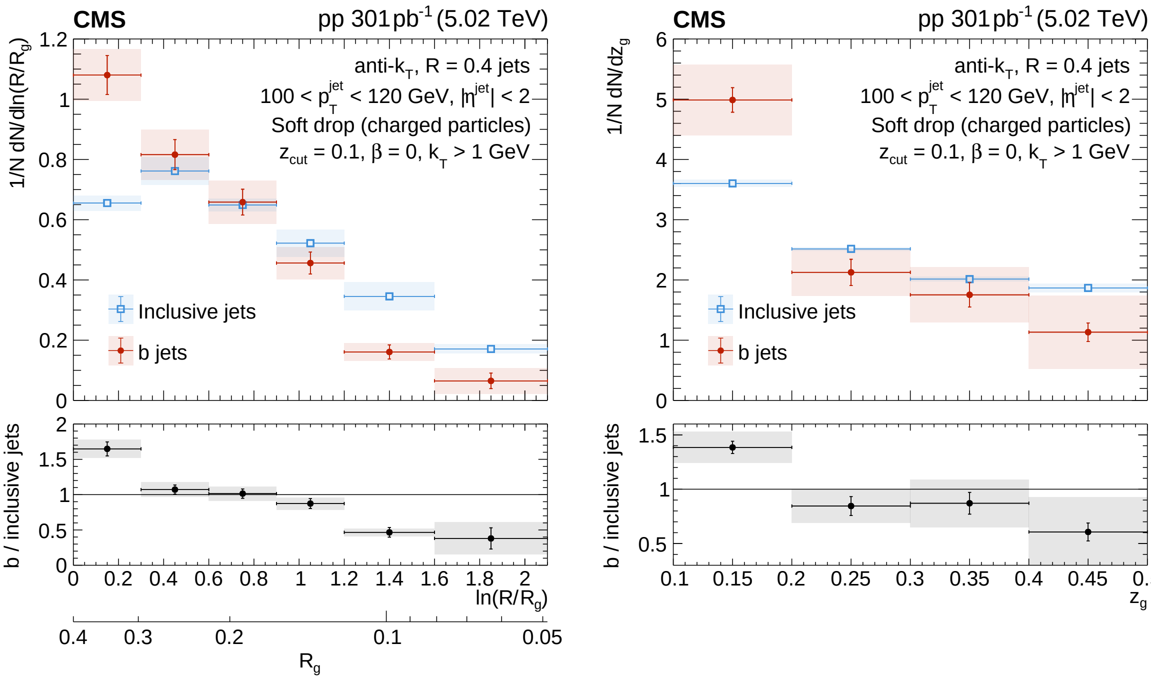

Figure 10: A comparison of the groomed observables R_g (left) and z_g (right) between b and inclusive jets. Most sources of systematic uncertainty are considered fully correlated in the ratio, which is presented in the lower panels, with the exception of those related to flavor and the response matrix.

diation pattern of b jets, the b hadron decay daughters need to be handled in a careful way experimentally. This measurement uses a novel algorithm to identify and cluster the b hadron charged decay daughters of b-tagged jets in a generic way, which allows for a cleaner interpretation of the measured substructure variable distributions in terms of the parton showering description.

The contributions from gluon, light-quark, charm quark jets, and jets originating from gluon splitting ($g \to b\bar{b}$) are subtracted from the measurements. The distributions are unfolded to the charged-particle level using unregularized unfolding. The correction to the charged-particle level accounts also for the removal of the particle-level biases that arise from the usage of b tagging.

The charged-particle-level distributions have uncertainties of the order of 5% and reaching up to 20% in certain bins. The dominant systematic uncertainty is related to the physics model (PYTHIA8 CP5 or HERWIG7 CH3) used in extraction of the corrections. The groomed momentum balance distributions of inclusive jets and b jets are well described by both PYTHIA8 CP5 and HERWIG7 CH3. The description of the groomed jet radius, however, depends on the jet flavor and the physics model. The HERWIG7 CH3 prediction agrees well with the data in the case of inclusive jets, while a bigger discrepancy is observed for b jets. The PYTHIA8 CP5 generator fails to describe either distribution. The jet fragmentation function, on the other hand, is described better by PYTHIA8 CP5 at high values of $z_{b,ch}$, i.e., for cases where the b hadron carries a substantial amount of the jet p_T. The $z_{b,ch} \approx 1$ region corresponds to b jets without splittings that satisfy the soft-drop condition.

Therefore, z_g, R_g, and $z_{b,ch}$ can be used simultaneously to constrain nonperturbative and perturbative aspects of b jet substructure. The R_g distribution for b jets is found to differ signifi-

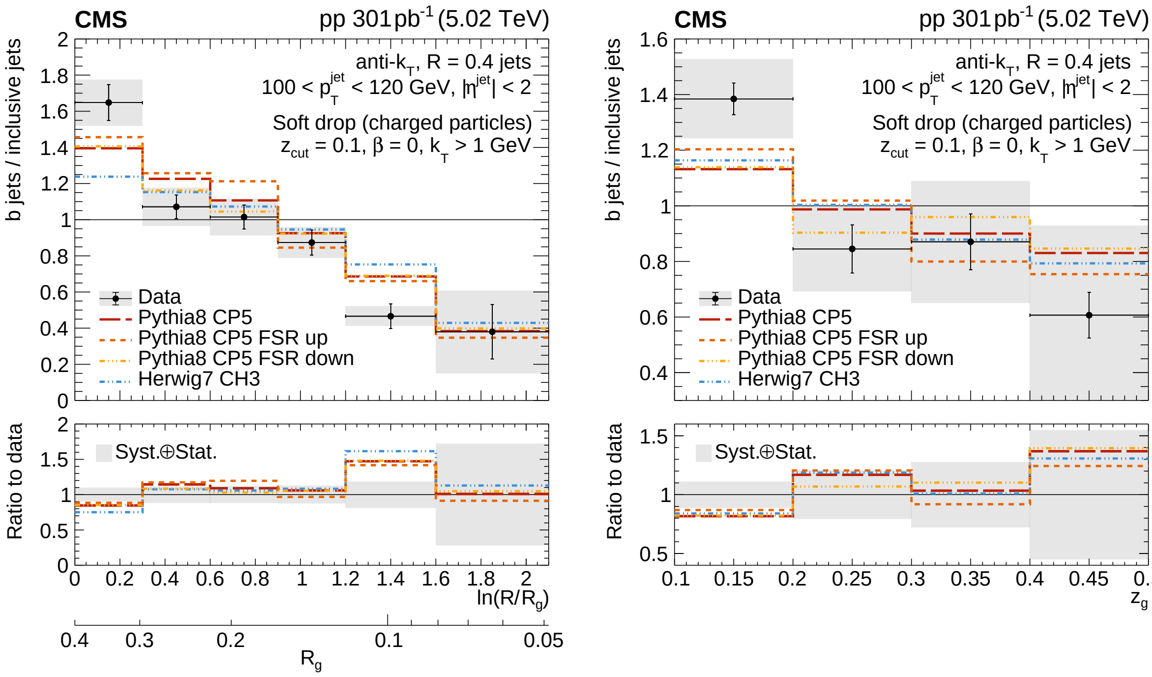

Figure 11: The ratio of the groomed observables R_g (left) and z_g (right) between b and inclusive jets compared to the PYTHIA8 CP5 and HERWIG7 CH3 MC event generators. Most sources of systematic uncertainty are considered fully correlated in the ratio, with the exception of those related to flavor and the response matrix. The ratio of the MC simulations to the data is presented in the lower panels.

cantly from that of inclusive jets. The suppression at small R_g for b jets is consistent with the expectations of the dead-cone effect. The b jets also have a more asymmetric z_g distribution than the inclusive jet reference, indicating that the b quark carries a greater amount of momentum when emitting gluons. The identified b quark dead cone may serve as a control region for isolated medium-induced radiation in Pb-Pb collisions in a future measurement.

Acknowledgments

We congratulate our colleagues in the CERN accelerator departments for the excellent performance of the LHC and thank the technical and administrative staffs at CERN and at other CMS institutes for their contributions to the success of the CMS effort. In addition, we gratefully acknowledge the computing centers and personnel of the Worldwide LHC Computing Grid and other centers for delivering so effectively the computing infrastructure essential to our analyses. Finally, we acknowledge the enduring support for the construction and operation of the LHC, the CMS detector, and the supporting computing infrastructure provided by the following funding agencies: SC (Armenia), BMBWF and FWF (Austria); FNRS and FWO (Belgium); CNPq, CAPES, FAPERJ, FAPERGS, and FAPESP (Brazil); MES and BNSF (Bulgaria); CERN; CAS, MoST, and NSFC (China); MINCIENCIAS (Colombia); MSES and CSF (Croatia); RIF (Cyprus); SENESCYT (Ecuador); ERC PRG, TARISTU24-TK10 and MoER TK202 (Estonia); Academy of Finland, MEC, and HIP (Finland); CEA and CNRS/IN2P3 (France); SRNSF (Georgia); BMFTR, DFG, and HGF (Germany); GSRI (Greece); NKFIH (Hungary); DAE and DST (India); IPM (Iran); SFI (Ireland); INFN (Italy); MSIT and NRF (Republic of Korea); MES (Latvia); LMTLT (Lithuania); MOE and UM (Malaysia); BUAP, CINVESTAV, CONACYT, LNS, SEP, and UASLP-FAI (Mexico); MOS (Montenegro); MBIE (New Zealand); PAEC (Pakistan);

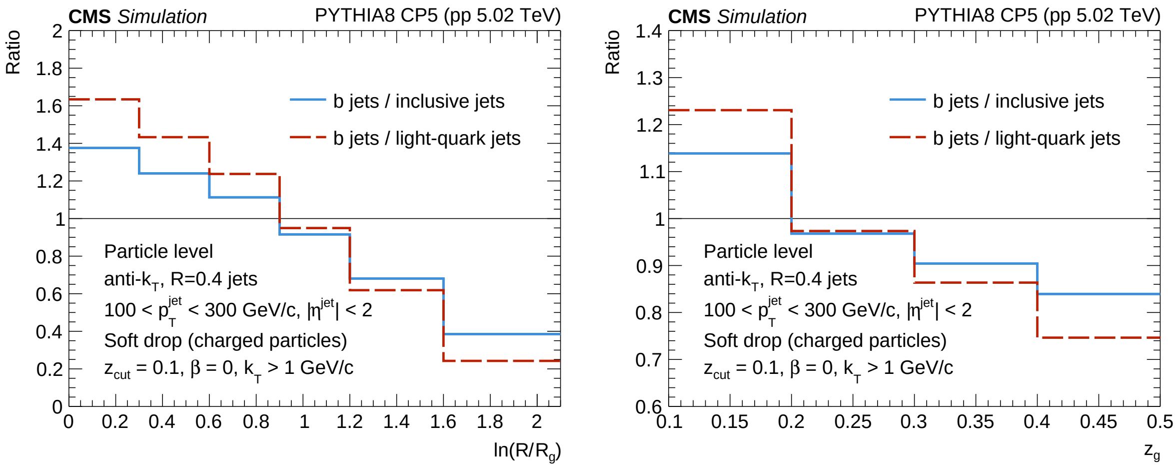

Figure 12: The ratio of the groomed observables R_g (left) and z_g (right) between b and light-quark (dashed red line) or inclusive jets (solid blue line) at the particle level of the PYTHIA8 CP5 event generator.

MES, NSC, and NAWA (Poland); FCT (Portugal); MESTD (Serbia); MICIU/AEI and PCTI (Spain); MOSTR (Sri Lanka); Swiss Funding Agencies (Switzerland); MST (Taipei); MHESI (Thailand); TUBITAK and TENMAK (Türkiye); NASU (Ukraine); STFC (United Kingdom); DOE and NSF (USA).

Individuals have received support from the Marie-Curie program and the European Research Council and Horizon 2020 Grant, contract Nos. 675440, 724704, 752730, 758316, 765710, 824093, 101115353, 101002207, 101001205, and COST Action CA16108 (European Union); the Leventis Foundation; the Alfred P. Sloan Foundation; the Alexander von Humboldt Foundation; the Science Committee, project no. 22rl-037 (Armenia); the Fonds pour la Formation à la Recherche dans l'Industrie et dans l'Agriculture (FRIA) and Fonds voor Wetenschappelijk Onderzoek contract No. 1228724N (Belgium); the Beijing Municipal Science & Technology Commission, No. Z191100007219010, the Fundamental Research Funds for the Central Universities, the Ministry of Science and Technology of China under Grant No. 2023YFA1605804, the Natural Science Foundation of China under Grant No. 12061141002, 12535004, and USTC Research Funds of the Double First-Class Initiative No. YD2030002017 (China); the Ministry of Education, Youth and Sports (MEYS) of the Czech Republic; the Shota Rustaveli National Science Foundation, grant FR-22-985 (Georgia); the Deutsche Forschungsgemeinschaft (DFG), among others, under Germany's Excellence Strategy – EXC 2121 "Quantum Universe" – 390833306, and under project number 400140256 - GRK2497; the Hellenic Foundation for Research and Innovation (HFRI), Project Number 2288 (Greece); the Hungarian Academy of Sciences, the New National Excellence Program - ÚNKP, the NKFIH research grants K 131991, K 133046, K 138136, K 143460, K 143477, K 146913, K 146914, K 147048, 2020-2.2.1-ED-2021-00181, TKP2021-NKTA-64, and 2021-4.1.2-NEMZ_KI-2024-00036 (Hungary); the Council of Science and Industrial Research, India; ICSC – National Research Center for High Performance Computing, Big Data and Quantum Computing, FAIR – Future Artificial Intelligence Research, and CUP I53D23001070006 (Mission 4 Component 1), funded by the NextGenerationEU program (Italy); the Latvian Council of Science; the Ministry of Education and Science, project no. 2022/WK/14, and the National Science Center, contracts Opus 2021/41/B/ST2/01369, 2021/43/B/ST2/01552, 2023/49/B/ST2/03273, and the NAWA contract BPN/PPO/2021/1/00011 (Poland); the Fundação para a Ciência e a Tecnologia, grant CEECIND/01334/2018 (Portugal); the National Priorities Research Program by Qatar National

Research Fund; MICIU/AEI/10.13039/501100011033, ERDF/EU, "European Union NextGenerationEU/PRTR", and Programa Severo Ochoa del Principado de Asturias (Spain); the Chulalongkorn Academic into Its 2nd Century Project Advancement Project, the National Science, Research and Innovation Fund program IND_FF_68_369_2300_097, and the Program Management Unit for Human Resources & Institutional Development, Research and Innovation, grant B39G680009 (Thailand); the Kavli Foundation; the Nvidia Corporation; the SuperMicro Corporation; the Welch Foundation, contract C-1845; and the Weston Havens Foundation (USA).

References

[1] A. J. Larkoski, I. Moult, and B. Nachman, "Jet substructure at the Large Hadron Collider: a review of recent advances in theory and machine learning", *Phys. Rept.* **841** (2020) 1, doi:10.1016/j.physrep.2019.11.001, arXiv:1709.04464.

[2] S. Marzani, G. Soyez, and M. Spannowsky, "Looking inside jets: an introduction to jet substructure and boosted-object phenomenology", *Lect. Notes Phys.* **958** (2019) 1, doi:10.1007/978-3-030-15709-8, arXiv:1901.10342.

[3] R. Kogler, "Advances in jet substructure at the LHC: algorithms, measurements and searches for new physical phenomena", volume 284 of *Springer Tracts Mod. Phys.* Springer, 2021. doi:10.1007/978-3-030-72858-8, ISBN 978-3-030-72857-1, 978-3-030-72858-8.

[4] V. N. Gribov and L. N. Lipatov, "Deep inelastic electron-proton scattering in perturbation theory", *Sov. J. Nucl. Phys.* **15** (1972) 438.

[5] Y. L. Dokshitzer, "Calculation of the structure functions for deep inelastic scattering and e^+e^- annihilation by perturbation theory in quantum chromodynamics", *Sov. Phys. JETP* **46** (1977) 641.

[6] G. Altarelli and G. Parisi, "Asymptotic freedom in parton language", *Nucl. Phys. B* **126** (1977) 298, doi:10.1016/0550-3213(77)90384-4.

[7] S. Catani, S. Dittmaier, and Z. Trocsanyi, "One loop singular behavior of QCD and SUSY QCD amplitudes with massive partons", *Phys. Lett. B* **500** (2001) 149, doi:10.1016/S0370-2693(01)00065-X, arXiv:hep-ph/0011222.

[8] P. Ilten, N. L. Rodd, J. Thaler, and M. Williams, "Disentangling heavy flavor at colliders", *Phys. Rev. D* **96** (2017) 054019, doi:10.1103/PhysRevD.96.054019, arXiv:1702.02947.

[9] Y. L. Dokshitzer, V. A. Khoze, and S. I. Troian, "On specific QCD properties of heavy quark fragmentation ('dead cone')", *J. Phys. G* **17** (1991) 1602, doi:10.1088/0954-3899/17/10/023.

[10] ALICE Collaboration, "Direct observation of the dead-cone effect in quantum chromodynamics", *Nature* **605** (2022) 440, doi:10.1038/s41586-022-04572-w, arXiv:2106.05713. [Erratum: doi:10.1038/s41586-022-05026-z].

[11] CMS Collaboration, "Identification of heavy-flavor jets with the CMS detector in pp collisions at 13 TeV", *JINST* **13** (2018) P05011, doi:10.1088/1748-0221/13/05/P05011, arXiv:1712.07158.

[12] R. Kogler, B. Nachman, A. Schmidt (editors) and others, "Jet substructure at the Large Hadron Collider: experimental review", *Rev. Mod. Phys.* **91** (2019) 045003, doi:10.1103/RevModPhys.91.045003, arXiv:1803.06991.

[13] CMS Collaboration, "Evidence of b jet quenching in PbPb collisions at $\sqrt{s_{_{\mathrm{NN}}}} = 2.76\,\mathrm{TeV}$", *Phys. Rev. Lett.* **113** (2014) 132301, doi:10.1103/PhysRevLett.113.132301, arXiv:1312.4198. [Erratum: doi:10.1103/PhysRevLett.115.029903].

[14] ATLAS Collaboration, "Measurement of the nuclear modification factor of b jets in 5.02 TeV PbPb collisions with the ATLAS detector", *Eur. Phys. J. C* **83** (2023) 438, doi:10.1140/epjc/s10052-023-11427-9, arXiv:2204.13530.

[15] CMS Collaboration, "Comparing transverse momentum balance of b jet pairs in pp and PbPb collisions at $\sqrt{s_{_{\mathrm{NN}}}} = 5.02\,\mathrm{TeV}$", *JHEP* **03** (2018) 181, doi:10.1007/JHEP03(2018)181, arXiv:1802.00707.

[16] CMS Collaboration, "Overview of high-density QCD studies with the CMS experiment at the LHC", *Phys. Rept.* **1115** (2025) 219, doi:10.1016/j.physrep.2024.11.007, arXiv:2405.10785.

[17] L. Cunqueiro and M. Płoskoń, "Searching for the dead-cone effects with iterative declustering of heavy-flavor jets", *Phys. Rev. D* **99** (2019) 074027, doi:10.1103/PhysRevD.99.074027, arXiv:1812.00102.

[18] L. Cunqueiro, D. Napoletano, and A. Soto-Ontoso, "Dead-cone searches in heavy-ion collisions using the jet tree", *Phys. Rev. D* **107** (2023) 094008, doi:10.1103/PhysRevD.107.094008, arXiv:2211.11789.

[19] CMS Collaboration, "Search for medium effects using jets from bottom quarks in PbPb collisions at $\sqrt{s_{NN}} = 5.02\,\mathrm{TeV}$", *Phys. Lett. B* **844** (2023) 137849, doi:10.1016/j.physletb.2023.137849, arXiv:2210.08547.

[20] C. Lee, P. Shrivastava, and V. Vaidya, "Predictions for energy correlators probing substructure of groomed heavy-quark jets", *JHEP* **09** (2019) 045, doi:10.1007/JHEP09(2019)045, arXiv:1901.09095.

[21] DELPHI Collaboration, "A study of the b-quark fragmentation function with the DELPHI detector at LEP I and an averaged distribution obtained at the Z pole", *Eur. Phys. J. C* **71** (2011) 1557, doi:10.1140/epjc/s10052-011-1557-x, arXiv:1102.4748.

[22] OPAL Collaboration, "Inclusive analysis of the b quark fragmentation function in Z decays at LEP", *Eur. Phys. J. C* **29** (2003) 463, doi:10.1140/epjc/s2003-01229-x, arXiv:hep-ex/0210031.

[23] S. Kluth, W. Ochs, and R. Perez Ramos, "Observation of the dead-cone effect in charm and bottom quark jets and its QCD explanation", *Phys. Rev. D* **107** (2023) 094039, doi:10.1103/PhysRevD.107.094039, arXiv:2303.13343.

[24] A. J. Larkoski, S. Marzani, G. Soyez, and J. Thaler, "Soft drop", *JHEP* **05** (2014) 146, doi:10.1007/JHEP05(2014)146, arXiv:1402.2657.

[25] M. Dasgupta, A. Fregoso, S. Marzani, and G. P. Salam, "Towards an understanding of jet substructure", *JHEP* **09** (2013) 029, doi:10.1007/JHEP09(2013)029, arXiv:1307.0007.

[26] Y. L. Dokshitzer, G. D. Leder, S. Moretti, and B. R. Webber, "Better jet clustering algorithms", *JHEP* **08** (1997) 001, doi:10.1088/1126-6708/1997/08/001, arXiv:hep-ph/9707323.

[27] S. Caletti, A. Ghira, and S. Marzani, "On heavy-flavor jets with soft drop", *Eur. Phys. J. C* **84** (2024) 212, doi:10.1140/epjc/s10052-024-12562-7, arXiv:2312.11623.

[28] ALEPH Collaboration, "Study of the fragmentation of b quarks into B mesons at the Z peak", *Phys. Lett. B* **512** (2001) 30, doi:10.1016/S0370-2693(01)00690-6, arXiv:hep-ex/0106051.

[29] ATLAS Collaboration, "Measurement of b-quark fragmentation properties in jets using the decay $B^{\pm} \rightarrow J/\psi K^{\pm}$ in pp collisions at $\sqrt{s} = 13\,\text{TeV}$ with the ATLAS detector", *JHEP* **12** (2021) 131, doi:10.1007/JHEP12(2021)131, arXiv:2108.11650.

[30] ATLAS Collaboration, "Measurements of jet observables sensitive to b-quark fragmentation in $\mathrm{t\bar{t}}$ events at the LHC with the ATLAS detector", *Phys. Rev. D* **106** (2022) 032008, doi:10.1103/PhysRevD.106.032008, arXiv:2202.13901.

[31] HEPData record for this analysis, 2025. doi:10.17182/hepdata.156184.

[32] CMS Collaboration, "The CMS experiment at the CERN LHC", *JINST* **3** (2008) S08004, doi:10.1088/1748-0221/3/08/S08004.

[33] CMS Collaboration, "Development of the CMS detector for the CERN LHC Run 3", *JINST* **19** (2024), no. 05, P05064, doi:10.1088/1748-0221/19/05/P05064, arXiv:2309.05466.

[34] CMS Collaboration, "Technical proposal for the Phase-2 upgrade of the Compact Muon Solenoid", CMS Technical Proposal CERN-LHCC-2015-010, CMS-TDR-15-02, 2015. doi:10.17181/CERN.VU8I.D59J.

[35] A. M. Sirunyan et al., "Particle-flow reconstruction and global event description with the CMS detector", *JINST* **12** (2017) P10003, doi:10.1088/1748-0221/12/10/P10003, arXiv:1706.04965.

[36] M. Cacciari, G. P. Salam, and G. Soyez, "The anti-k_{T} jet clustering algorithm", *JHEP* **04** (2008) 063, doi:10.1088/1126-6708/2008/04/063, arXiv:0802.1189.

[37] M. Cacciari, G. P. Salam, and G. Soyez, "FastJet user manual", *Eur. Phys. J. C* **72** (2012) 1896, doi:10.1140/epjc/s10052-012-1896-2, arXiv:1111.6097.

[38] CMS Collaboration, "Pileup mitigation at CMS in 13 TeV data", *JINST* **15** (2020) P09018, doi:10.1088/1748-0221/15/09/P09018, arXiv:2003.00503.

[39] CMS Collaboration, "Jet energy scale and resolution in the CMS experiment in pp collisions at 8 TeV", *JINST* **12** (2017) P02014, doi:10.1088/1748-0221/12/02/P02014, arXiv:1607.03663.

[40] H. Qu and L. Gouskos, "ParticleNet: jet tagging via particle clouds", *Phys. Rev. D* **101** (2020), no. 5, 056019, doi:10.1103/PhysRevD.101.056019, arXiv:1902.08570.

[41] CMS Tracker Group, "The CMS Phase-1 pixel detector upgrade", *JINST* **16** (2021) P02027, doi:10.1088/1748-0221/16/02/P02027, arXiv:2012.14304.

[42] CMS Collaboration, “Track impact parameter resolution for the full pseudorapidity coverage in the 2017 dataset with the CMS Phase-1 pixel detector”, CMS Detector Performance Note CMS-DP-2020-049, 2020.

[43] CMS Collaboration, “Performance of the CMS Level-1 trigger in proton-proton collisions at $\sqrt{s} = 13\,\text{TeV}$”, *JINST* **15** (2020) P10017, doi:10.1088/1748-0221/15/10/P10017, arXiv:2006.10165.

[44] CMS Collaboration, “The CMS trigger system”, *JINST* **12** (2017) P01020, doi:10.1088/1748-0221/12/01/P01020, arXiv:1609.02366.

[45] CMS Collaboration, “Luminosity measurement in proton-proton collisions at 5.02 TeV in 2017 at CMS”, CMS Physics Analysis Summary CMS-PAS-LUM-19-001, 2021.

[46] T. Sjöstrand et al., “An introduction to PYTHIA8.2”, *Comput. Phys. Commun.* **191** (2015) 159, doi:10.1016/j.cpc.2015.01.024, arXiv:1410.3012.

[47] CMS Collaboration, “Extraction and validation of a new set of CMS PYTHIA8 tunes from underlying-event measurements”, *Eur. Phys. J. C* **80** (2020) 4, doi:10.1140/epjc/s10052-019-7499-4, arXiv:1903.12179.

[48] E. Norrbin and T. Sjöstrand, “QCD radiation off heavy particles”, *Nucl. Phys. B* **603** (2001) 297, doi:10.1016/S0550-3213(01)00099-2, arXiv:hep-ph/0010012.

[49] C. Bierlich et al., “A comprehensive guide to the physics and usage of PYTHIA8.3”, *SciPost Phys. Codeb.* **2022** (2022) 8, doi:10.21468/SciPostPhysCodeb.8, arXiv:2203.11601.

[50] B. Andersson, G. Gustafson, G. Ingelman, and T. Sjöstrand, “Parton fragmentation and string dynamics”, *Phys. Rept.* **97** (1983) 31, doi:10.1016/0370-1573(83)90080-7.

[51] T. Sjöstrand, “The merging of jets”, *Phys. Lett. B* **142** (1984) 420, doi:10.1016/0370-2693(84)91354-6.

[52] M. G. Bowler, “e^+e^- production of heavy quarks in the string model”, *Z. Phys. C* **11** (1981) 169, doi:10.1007/BF01574001.

[53] J. Bellm et al., “HERWIG7.1 Release Note”, 2017. arXiv:1705.06919.

[54] CMS Collaboration, “Development and validation of HERWIG7 tunes from CMS underlying-event measurements”, *Eur. Phys. J. C* **81** (2021) 312, doi:10.1140/epjc/s10052-021-08949-5, arXiv:2011.03422.

[55] S. Gieseke, P. Stephens, and B. Webber, “New formalism for QCD parton showers”, *JHEP* **12** (2003) 045, doi:10.1088/1126-6708/2003/12/045, arXiv:hep-ph/0310083.

[56] G. Marchesini and B. R. Webber, “Simulation of QCD coherence in heavy quark production and decay”, *Nucl. Phys. B* **330** (1990) 261, doi:10.1016/0550-3213(90)90310-A.

[57] B. R. Webber, “A QCD model for jet fragmentation including soft gluon interference”, *Nucl. Phys. B* **238** (1984) 492, doi:10.1016/0550-3213(84)90333-X.

[58] NNPDF Collaboration, “Parton distributions for the LHC Run 2”, *JHEP* **04** (2015) 040, doi:10.1007/JHEP04(2015)040, arXiv:1410.8849.

[59] GEANT4 Collaboration, “GEANT4—a simulation toolkit”, *Nucl. Instrum. Meth. A* **506** (2003) 250, `doi:10.1016/S0168-9002(03)01368-8`.

[60] M. Wobisch and T. Wengler, “Hadronization corrections to jet cross sections in deep inelastic scattering”, in *Workshop on Monte Carlo generators for HERA physics*, p. 270. 1998. `arXiv:hep-ph/9907280`. `doi:10.48550/arXiv.hep-ph/9907280`.

[61] F. A. Dreyer, G. P. Salam, and G. Soyez, “The Lund jet plane”, *JHEP* **12** (2018) 064, `doi:10.1007/JHEP12(2018)064`, `arXiv:1807.04758`.

[62] ALICE Collaboration, “Measurement of the groomed jet radius and momentum splitting fraction in pp and PbPb collisions at $\sqrt{s_{NN}} = 5.02$ TeV”, *Phys. Rev. Lett.* **128** (2022) 102001, `doi:10.1103/PhysRevLett.128.102001`, `arXiv:2107.12984`.

[63] ATLAS Collaboration, “Measurement of soft-drop jet observables in pp collisions with the ATLAS detector at $\sqrt{s} = 13$ TeV”, *Phys. Rev. D* **101** (2020) 052007, `doi:10.1103/PhysRevD.101.052007`, `arXiv:1912.09837`.

[64] CMS Collaboration, “Study of quark and gluon jet substructure in Z+jet and dijet events from pp collisions”, *JHEP* **01** (2022) 188, `doi:10.1007/JHEP01(2022)188`, `arXiv:2109.03340`.

[65] CMS Collaboration, “Measurements of the differential jet cross section as a function of the jet mass in dijet events from proton-proton collisions at $\sqrt{s} = 13$ TeV”, *JHEP* **11** (2018) 113, `doi:10.1007/JHEP11(2018)113`, `arXiv:1807.05974`.

[66] ATLAS Collaboration, “Measurement of jet-substructure observables in top quark, W boson and light jet production in proton-proton collisions at $\sqrt{s} = 13$ TeV with the ATLAS detector”, *JHEP* **08** (2019) 033, `doi:10.1007/JHEP08(2019)033`, `arXiv:1903.02942`.

[67] ATLAS Collaboration, “Measurements of Lund subjet multiplicities in 13 TeV proton-proton collisions with the ATLAS detector”, *Phys. Lett. B* **859** (2024) 139090, `doi:10.1016/j.physletb.2024.139090`, `arXiv:2402.13052`.

[68] ATLAS Collaboration, “Measurement of the Lund jet plane using charged particles in 13 TeV proton-proton collisions with the ATLAS detector”, *Phys. Rev. Lett.* **124** (2020) 222002, `doi:10.1103/PhysRevLett.124.222002`, `arXiv:2004.03540`.

[69] CMS Collaboration, “Measurement of the primary Lund jet plane density in proton-proton collisions at $\sqrt{s} = 13$ TeV”, *JHEP* **05** (2024) 116, `doi:10.1007/JHEP05(2024)116`, `arXiv:2312.16343`.

[70] ATLAS Collaboration, “Measurement of the Lund jet plane in hadronic decays of top quarks and W bosons with the ATLAS detector”, *Eur. Phys. J. C* **85** (2025), no. 4, 416, `doi:10.1140/epjc/s10052-025-13924-5`, `arXiv:2407.10879`.

[71] ALICE Collaboration, “Measurements of groomed-jet substructure of charm jets tagged by D0 mesons in proton-proton collisions at $\sqrt{s} = 13$ TeV”, *Phys. Rev. Lett.* **131** (2023) 192301, `doi:10.1103/PhysRevLett.131.192301`, `arXiv:2208.04857`.

[72] Particle Data Group Collaboration, “Review of particle physics”, *Phys. Rev. D* **110** (2024) 030001, `doi:10.1103/PhysRevD.110.030001`.

[73] CMS Collaboration, "Measurement of jet substructure observables in $\mathrm{t\bar{t}}$ events from proton-proton collisions at $\sqrt{s} = 13\,\mathrm{TeV}$", *Phys. Rev. D* **98** (2018) 092014, doi:10.1103/PhysRevD.98.092014, arXiv:1808.07340.

[74] CMS Collaboration, "Measurement of b jet shapes in proton-proton collisions at $\sqrt{s} = 5.02\,\mathrm{TeV}$", *JHEP* **05** (2021) 054, doi:10.1007/JHEP05(2021)054, arXiv:2005.14219.

[75] LHCb Collaboration, "Study of J/ψ production in jets", *Phys. Rev. Lett.* **118** (2017) 192001, doi:10.1103/PhysRevLett.118.192001, arXiv:1701.05116.

[76] CMS Collaboration, "Identification of b quark jets with the CMS experiment", *JINST* **8** (2013) P04013, doi:10.1088/1748-0221/8/04/P04013, arXiv:1211.4462.

[77] L. Brenner et al., "Comparison of unfolding methods using RooFitUnfold", *Int. J. Mod. Phys. A* **35** (2020) 2050145, doi:10.1142/S0217751X20501456, arXiv:1910.14654.

[78] T. Adye, "Unfolding algorithms and tests using RooUnfold", in *PHYSTAT 2011*, p. 313. CERN, Geneva, 2011. arXiv:1105.1160. doi:10.5170/CERN-2011-006.313.

[79] M. Cacciari et al., "The $\mathrm{t\bar{t}}$ cross section at 1.8 TeV and 1.96 TeV: a study of the systematics due to parton densities and scale dependence", *JHEP* **04** (2004) 068, doi:10.1088/1126-6708/2004/04/068, arXiv:hep-ph/0303085.

[80] S. Catani, D. de Florian, M. Grazzini, and P. Nason, "Soft-gluon resummation for Higgs boson production at hadron colliders", *JHEP* **07** (2003) 028, doi:10.1088/1126-6708/2003/07/028, arXiv:hep-ph/0306211.

[81] M. H. Quenouille, "Approximate tests of correlation in time-series", *J. Royal Stat. Soc. B* **11** (1949) 68, doi:10.1111/j.2517-6161.1949.tb00023.x.

[82] M. H. Quenouille, "Notes on bias in estimation", *Biometrika* **43** (1956) 353, doi:10.2307/2332914.

[83] R. G. Miller, "The jackknife—a review", *Biometrika* **61** (1974) 1, doi:10.2307/2334280.

A The b hadron decay product identification and clustering

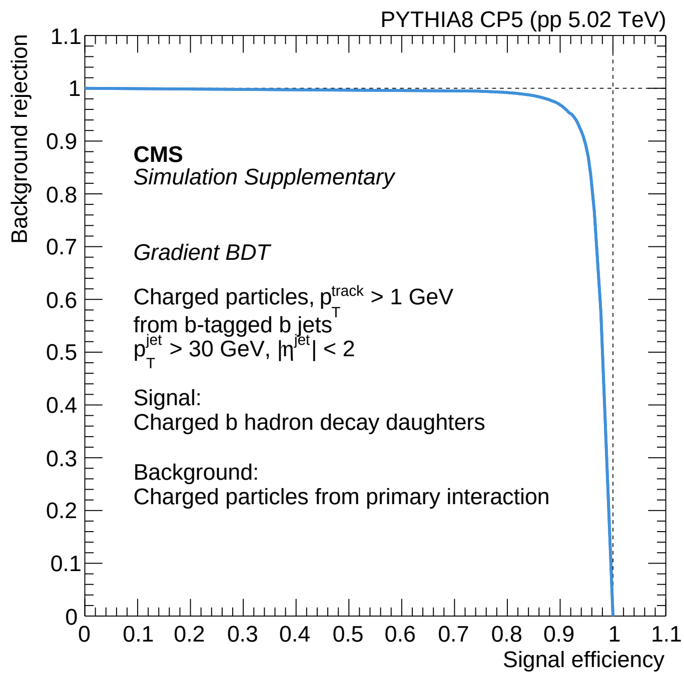

Figure A.1: The background rejection rate versus the signal efficiency for the b hadron decay product identification. The model is a gradient boosted decision tree with 11 input variables related to tracking and secondary vertex information. "Background" refers to charged particles coming from the primary interaction, while "signal" signifies charged particles resulting from a b hadron decay. Dashed lines are drawn at 1 for each axis. The intersection of those lines is the optimal performance of a classifier.

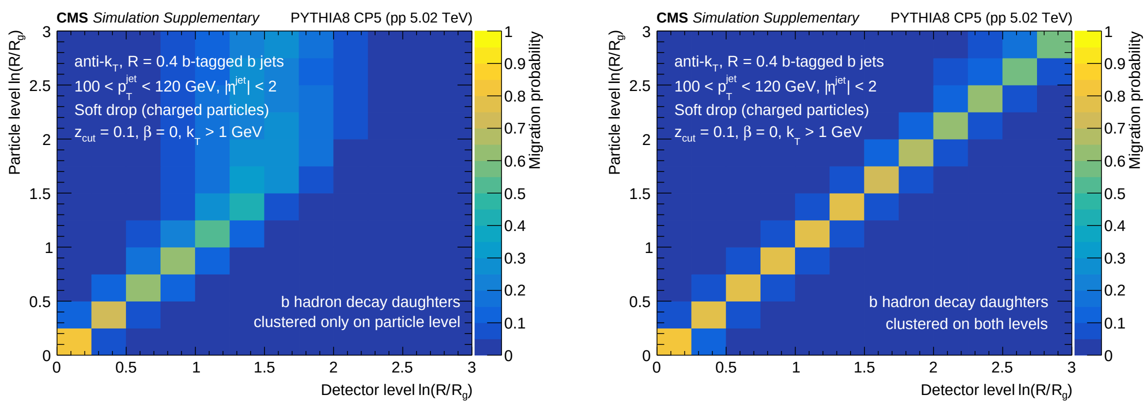

Figure A.2: The migration matrices of R_g for b jets. The particle level corresponds to clustered b hadron decay products. In the left panel, the decay products are present during the iterative declustering at the detector level, while in the right panel, the decay products have been identified using the gradient boosted decision tree and they have been clustered together into the partially reconstructed b hadron and replaced in the jet constituents.

B The CMS Collaboration

Yerevan Physics Institute, Yerevan, Armenia
V. Chekhovsky, A. Hayrapetyan, V. Makarenko, A. Tumasyan[1]

Institut für Hochenergiephysik, Vienna, Austria
W. Adam, J.W. Andrejkovic, L. Benato, T. Bergauer, S. Chatterjee, K. Damanakis, M. Dragicevic, P.S. Hussain, M. Jeitler[2], N. Krammer, A. Li, D. Liko, I. Mikulec, J. Schieck[2], R. Schöfbeck[2], D. Schwarz, M. Sonawane, W. Waltenberger, C.-E. Wulz[2]

Universiteit Antwerpen, Antwerpen, Belgium
T. Janssen, H. Kwon, T. Van Laer, P. Van Mechelen

Vrije Universiteit Brussel, Brussel, Belgium
N. Breugelmans, J. D'Hondt, S. Dansana, A. De Moor, M. Delcourt, F. Heyen, Y. Hong, S. Lowette, I. Makarenko, D. Müller, S. Tavernier, M. Tytgat[3], G.P. Van Onsem, S. Van Putte, D. Vannerom

Université Libre de Bruxelles, Bruxelles, Belgium
B. Bilin, B. Clerbaux, A.K. Das, I. De Bruyn, G. De Lentdecker, H. Evard, L. Favart, P. Gianneios, A. Khalilzadeh, F.A. Khan, A. Malara, M.A. Shahzad, L. Thomas, M. Vanden Bemden, C. Vander Velde, P. Vanlaer

Ghent University, Ghent, Belgium
M. De Coen, D. Dobur, G. Gokbulut, J. Knolle, L. Lambrecht, D. Marckx, K. Skovpen, N. Van Den Bossche, J. van der Linden, J. Vandenbroeck, L. Wezenbeek

Université Catholique de Louvain, Louvain-la-Neuve, Belgium
S. Bein, A. Benecke, A. Bethani, G. Bruno, C. Caputo, J. De Favereau De Jeneret, C. Delaere, I.S. Donertas, A. Giammanco, A.O. Guzel, Sa. Jain, V. Lemaitre, J. Lidrych, P. Mastrapasqua, T.T. Tran, S. Turkcapar

Centro Brasileiro de Pesquisas Fisicas, Rio de Janeiro, Brazil
G.A. Alves, E. Coelho, G. Correia Silva, C. Hensel, T. Menezes De Oliveira, C. Mora Herrera[4], P. Rebello Teles, M. Soeiro, E.J. Tonelli Manganote[5], A. Vilela Pereira[4]

Universidade do Estado do Rio de Janeiro, Rio de Janeiro, Brazil
W.L. Aldá Júnior, M. Barroso Ferreira Filho, H. Brandao Malbouisson, W. Carvalho, J. Chinellato[6], E.M. Da Costa, G.G. Da Silveira[7], D. De Jesus Damiao, S. Fonseca De Souza, R. Gomes De Souza, T. Laux Kuhn[7], M. Macedo, J. Martins, K. Mota Amarilo, L. Mundim, H. Nogima, J.P. Pinheiro, A. Santoro, A. Sznajder, M. Thiel

Universidade Estadual Paulista, Universidade Federal do ABC, São Paulo, Brazil
C.A. Bernardes[7], L. Calligaris, T.R. Fernandez Perez Tomei, E.M. Gregores, I. Maietto Silverio, P.G. Mercadante, S.F. Novaes, B. Orzari, Sandra S. Padula, V. Scheurer

Institute for Nuclear Research and Nuclear Energy, Bulgarian Academy of Sciences, Sofia, Bulgaria
A. Aleksandrov, G. Antchev, R. Hadjiiska, P. Iaydjiev, M. Misheva, M. Shopova, G. Sultanov

University of Sofia, Sofia, Bulgaria
A. Dimitrov, L. Litov, B. Pavlov, P. Petkov, A. Petrov, E. Shumka

Instituto De Alta Investigación, Universidad de Tarapacá, Casilla 7 D, Arica, Chile
S. Keshri, D. Laroze, S. Thakur

Beihang University, Beijing, China
T. Cheng, T. Javaid, L. Yuan

Department of Physics, Tsinghua University, Beijing, China
Z. Hu, Z. Liang, J. Liu

Institute of High Energy Physics, Beijing, China
G.M. Chen[8], H.S. Chen[8], M. Chen[8], F. Iemmi, C.H. Jiang, A. Kapoor[9], H. Liao, Z.-A. Liu[10], R. Sharma[11], J.N. Song[10], J. Tao, C. Wang[8], J. Wang, Z. Wang[8], H. Zhang, J. Zhao

State Key Laboratory of Nuclear Physics and Technology, Peking University, Beijing, China
A. Agapitos, Y. Ban, A. Carvalho Antunes De Oliveira, S. Deng, B. Guo, C. Jiang, A. Levin, C. Li, Q. Li, Y. Mao, S. Qian, S.J. Qian, X. Qin, X. Sun, D. Wang, H. Yang, Y. Zhao, C. Zhou

State Key Laboratory of Nuclear Physics and Technology, Institute of Quantum Matter, South China Normal University, Guangzhou, China
S. Yang

Sun Yat-Sen University, Guangzhou, China
Z. You

University of Science and Technology of China, Hefei, China
K. Jaffel, N. Lu

Nanjing Normal University, Nanjing, China
G. Bauer[12], B. Li[13], H. Wang, K. Yi[14], J. Zhang

Institute of Modern Physics and Key Laboratory of Nuclear Physics and Ion-beam Application (MOE) - Fudan University, Shanghai, China
Y. Li

Zhejiang University, Hangzhou, Zhejiang, China
Z. Lin, C. Lu, M. Xiao

Universidad de Los Andes, Bogota, Colombia
C. Avila, D.A. Barbosa Trujillo, A. Cabrera, C. Florez, J. Fraga, J.A. Reyes Vega

Universidad de Antioquia, Medellin, Colombia
J. Jaramillo, C. Rendón, M. Rodriguez, A.A. Ruales Barbosa, J.D. Ruiz Alvarez

University of Split, Faculty of Electrical Engineering, Mechanical Engineering and Naval Architecture, Split, Croatia
D. Giljanovic, N. Godinovic, D. Lelas, A. Sculac

University of Split, Faculty of Science, Split, Croatia
M. Kovac, A. Petkovic, T. Sculac

Institute Rudjer Boskovic, Zagreb, Croatia
P. Bargassa, V. Brigljevic, B.K. Chitroda, D. Ferencek, K. Jakovcic, A. Starodumov[15],

T. Susa

University of Cyprus, Nicosia, Cyprus
A. Attikis, K. Christoforou, A. Hadjiagapiou, C. Leonidou, J. Mousa, C. Nicolaou, L. Paizanos, F. Ptochos, P.A. Razis, H. Rykaczewski, H. Saka, A. Stepennov

Charles University, Prague, Czech Republic
M. Finger, M. Finger Jr., A. Kveton

Escuela Politecnica Nacional, Quito, Ecuador
E. Ayala

Universidad San Francisco de Quito, Quito, Ecuador
E. Carrera Jarrin

Academy of Scientific Research and Technology of the Arab Republic of Egypt, Egyptian Network of High Energy Physics, Cairo, Egypt
H. Abdalla[16], R. Aly[17], Y. Assran[18,19]

Center for High Energy Physics (CHEP-FU), Fayoum University, El-Fayoum, Egypt
M. Abdullah Al-Mashad, M.A. Mahmoud

National Institute of Chemical Physics and Biophysics, Tallinn, Estonia
K. Ehataht, M. Kadastik, T. Lange, C. Nielsen, J. Pata, M. Raidal, L. Tani, C. Veelken

Department of Physics, University of Helsinki, Helsinki, Finland
K. Osterberg, M. Voutilainen

Helsinki Institute of Physics, Helsinki, Finland
N. Bin Norjoharuddeen, E. Brücken, F. Garcia, P. Inkaew, K.T.S. Kallonen, T. Lampén, K. Lassila-Perini, S. Lehti, T. Lindén, M. Myllymäki, M.m. Rantanen, J. Tuominiemi

Lappeenranta-Lahti University of Technology, Lappeenranta, Finland
H. Kirschenmann, P. Luukka, H. Petrow

IRFU, CEA, Université Paris-Saclay, Gif-sur-Yvette, France
M. Besancon, F. Couderc, M. Dejardin, D. Denegri, J.L. Faure, F. Ferri, S. Ganjour, P. Gras, G. Hamel de Monchenault, M. Kumar, V. Lohezic, J. Malcles, F. Orlandi, L. Portales, A. Rosowsky, M.Ö. Sahin, A. Savoy-Navarro[20], P. Simkina, M. Titov, M. Tornago

Laboratoire Leprince-Ringuet, CNRS/IN2P3, Ecole Polytechnique, Institut Polytechnique de Paris, Palaiseau, France
F. Beaudette, G. Boldrini, P. Busson, A. Cappati, C. Charlot, M. Chiusi, T.D. Cuisset, F. Damas, O. Davignon, A. De Wit, I.T. Ehle, B.A. Fontana Santos Alves, S. Ghosh, A. Gilbert, R. Granier de Cassagnac, B. Harikrishnan, L. Kalipoliti, G. Liu, M. Manoni, M. Nguyen, S. Obraztsov, C. Ochando, R. Salerno, J.B. Sauvan, Y. Sirois, G. Sokmen, L. Urda Gómez, E. Vernazza, A. Zabi, A. Zghiche

Université de Strasbourg, CNRS, IPHC UMR 7178, Strasbourg, France
J.-L. Agram[21], J. Andrea, D. Bloch, J.-M. Brom, E.C. Chabert, C. Collard, S. Falke, U. Goerlach, R. Haeberle, A.-C. Le Bihan, M. Meena, O. Poncet, G. Saha, M.A. Sessini, P. Van Hove, P. Vaucelle

Centre de Calcul de l'Institut National de Physique Nucleaire et de Physique des Particules, CNRS/IN2P3, Villeurbanne, France
A. Di Florio

Institut de Physique des 2 Infinis de Lyon (IP2I), Villeurbanne, France
D. Amram, S. Beauceron, B. Blancon, G. Boudoul, N. Chanon, D. Contardo, P. Depasse, C. Dozen[22], H. El Mamouni, J. Fay, S. Gascon, M. Gouzevitch, C. Greenberg, G. Grenier, B. Ille, E. Jourd'huy, I.B. Laktineh, M. Lethuillier, L. Mirabito, S. Perries, A. Purohit, M. Vander Donckt, P. Verdier, J. Xiao

Georgian Technical University, Tbilisi, Georgia
A. Khvedelidze[15], I. Lomidze, Z. Tsamalaidze[15]

RWTH Aachen University, I. Physikalisches Institut, Aachen, Germany
V. Botta, S. Consuegra Rodríguez, L. Feld, K. Klein, M. Lipinski, D. Meuser, A. Pauls, D. Pérez Adán, N. Röwert, M. Teroerde

RWTH Aachen University, III. Physikalisches Institut A, Aachen, Germany
S. Diekmann, A. Dodonova, N. Eich, D. Eliseev, F. Engelke, J. Erdmann, M. Erdmann, B. Fischer, T. Hebbeker, K. Hoepfner, F. Ivone, A. Jung, M.y. Lee, F. Mausolf, M. Merschmeyer, A. Meyer, F. Nowotny, A. Pozdnyakov, Y. Rath, W. Redjeb, F. Rehm, H. Reithler, V. Sarkisovi, A. Schmidt, C. Seth, A. Sharma, J.L. Spah, F. Torres Da Silva De Araujo[23], S. Wiedenbeck, S. Zaleski

RWTH Aachen University, III. Physikalisches Institut B, Aachen, Germany
C. Dziwok, G. Flügge, T. Kress, A. Nowack, O. Pooth, A. Stahl, T. Ziemons, A. Zotz

Deutsches Elektronen-Synchrotron, Hamburg, Germany
H. Aarup Petersen, M. Aldaya Martin, J. Alimena, S. Amoroso, Y. An, J. Bach, S. Baxter, M. Bayatmakou, H. Becerril Gonzalez, O. Behnke, A. Belvedere, F. Blekman[24], K. Borras[25], A. Campbell, A. Cardini, F. Colombina, M. De Silva, G. Eckerlin, D. Eckstein, L.I. Estevez Banos, E. Gallo[24], A. Geiser, V. Guglielmi, M. Guthoff, A. Hinzmann, L. Jeppe, B. Kaech, M. Kasemann, C. Kleinwort, R. Kogler, M. Komm, D. Krücker, W. Lange, D. Leyva Pernia, K. Lipka[26], W. Lohmann[27], F. Lorkowski, R. Mankel, I.-A. Melzer-Pellmann, M. Mendizabal Morentin, A.B. Meyer, G. Milella, K. Moral Figueroa, A. Mussgiller, L.P. Nair, J. Niedziela, A. Nürnberg, J. Park, E. Ranken, A. Raspereza, D. Rastorguev, J. Rübenach, L. Rygaard, M. Scham[28,25], S. Schnake[25], P. Schütze, C. Schwanenberger[24], D. Selivanova, K. Sharko, M. Shchedrolosiev, D. Stafford, F. Vazzoler, A. Ventura Barroso, R. Walsh, D. Wang, Q. Wang, K. Wichmann, L. Wiens[25], C. Wissing, Y. Yang, S. Zakharov, A. Zimermmane Castro Santos

University of Hamburg, Hamburg, Germany
A. Albrecht, S. Albrecht, M. Antonello, S. Bollweg, M. Bonanomi, P. Connor, K. El Morabit, Y. Fischer, E. Garutti, A. Grohsjean, J. Haller, D. Hundhausen, H.R. Jabusch, G. Kasieczka, P. Keicher, R. Klanner, W. Korcari, T. Kramer, C.c. Kuo, V. Kutzner, F. Labe, J. Lange, A. Lobanov, C. Matthies, L. Moureaux, M. Mrowietz, A. Nigamova, Y. Nissan, A. Paasch, K.J. Pena Rodriguez, T. Quadfasel, B. Raciti, M. Rieger, D. Savoiu, J. Schindler, P. Schleper, M. Schröder, J. Schwandt, M. Sommerhalder, H. Stadie, G. Steinbrück, A. Tews, B. Wiederspan, M. Wolf

Karlsruher Institut fuer Technologie, Karlsruhe, Germany
S. Brommer, E. Butz, T. Chwalek, A. Dierlamm, G.G. Dincer, U. Elicabuk, N. Faltermann, M. Giffels, A. Gottmann, F. Hartmann[29], R. Hofsaess, M. Horzela, U. Husemann, J. Kieseler, M. Klute, O. Lavoryk, J.M. Lawhorn, M. Link, A. Lintuluoto, S. Maier, M. Mormile, Th. Müller, M. Neukum, M. Oh, E. Pfeffer, M. Presilla, G. Quast, K. Rabbertz, B. Regnery, R. Schmieder, N. Shadskiy, I. Shvetsov, H.J. Simonis, L. Sowa, L. Stockmeier, K. Tauqeer, M. Toms, B. Topko, N. Trevisani, T. Voigtländer, R.F. Von Cube, J. Von Den Driesch, M. Wassmer, S. Wieland, F. Wittig, R. Wolf, X. Zuo

Institute of Nuclear and Particle Physics (INPP), NCSR Demokritos, Aghia Paraskevi, Greece
G. Anagnostou, G. Daskalakis, A. Kyriakis, A. Papadopoulos[29], A. Stakia

National and Kapodistrian University of Athens, Athens, Greece
G. Melachroinos, Z. Painesis, I. Paraskevas, N. Saoulidou, K. Theofilatos, E. Tziaferi, K. Vellidis, I. Zisopoulos

National Technical University of Athens, Athens, Greece
G. Bakas, T. Chatzistavrou, G. Karapostoli, K. Kousouris, I. Papakrivopoulos, E. Siamarkou, G. Tsipolitis

University of Ioánnina, Ioánnina, Greece
I. Bestintzanos, I. Evangelou, C. Foudas, C. Kamtsikis, P. Katsoulis, P. Kokkas, P.G. Kosmoglou Kioseoglou, N. Manthos, I. Papadopoulos, J. Strologas

HUN-REN Wigner Research Centre for Physics, Budapest, Hungary
C. Hajdu, D. Horvath[30,31], K. Márton, A.J. Rádl[32], F. Sikler, V. Veszpremi

MTA-ELTE Lendület CMS Particle and Nuclear Physics Group, Eötvös Loránd University, Budapest, Hungary
M. Csanád, K. Farkas, A. Fehérkuti[33], M.M.A. Gadallah[34], Á. Kadlecsik, P. Major, G. Pásztor, G.I. Veres

Faculty of Informatics, University of Debrecen, Debrecen, Hungary
B. Ujvari, G. Zilizi

HUN-REN ATOMKI - Institute of Nuclear Research, Debrecen, Hungary
G. Bencze, S. Czellar, J. Molnar, Z. Szillasi

Karoly Robert Campus, MATE Institute of Technology, Gyongyos, Hungary
T. Csorgo[33], F. Nemes[33], T. Novak

Panjab University, Chandigarh, India
S. Bansal, S.B. Beri, V. Bhatnagar, G. Chaudhary, S. Chauhan, N. Dhingra[35], A. Kaur, A. Kaur, H. Kaur, M. Kaur, S. Kumar, T. Sheokand, J.B. Singh, A. Singla

University of Delhi, Delhi, India
A. Bhardwaj, A. Chhetri, B.C. Choudhary, A. Kumar, A. Kumar, M. Naimuddin, K. Ranjan, M.K. Saini, S. Saumya

Indian Institute of Technology Kanpur, Kanpur, India
S. Mukherjee

Saha Institute of Nuclear Physics, HBNI, Kolkata, India

S. Baradia, S. Barman[36], S. Bhattacharya, S. Das Gupta, S. Dutta, S. Dutta, S. Sarkar

Indian Institute of Technology Madras, Madras, India
M.M. Ameen, P.K. Behera, S.C. Behera, S. Chatterjee, G. Dash, P. Jana, P. Kalbhor, S. Kamble, J.R. Komaragiri[37], D. Kumar[37], T. Mishra, B. Parida[38], P.R. Pujahari, N.R. Saha, A.K. Sikdar, R.K. Singh, P. Verma, S. Verma, A. Vijay

Tata Institute of Fundamental Research-A, Mumbai, India
S. Dugad, G.B. Mohanty, M. Shelake, P. Suryadevara

Tata Institute of Fundamental Research-B, Mumbai, India
A. Bala, S. Banerjee, S. Bhowmik[39], R.M. Chatterjee, M. Guchait, Sh. Jain, A. Jaiswal, B.M. Joshi, S. Kumar, G. Majumder, K. Mazumdar, S. Parolia, A. Thachayath

National Institute of Science Education and Research, An OCC of Homi Bhabha National Institute, Bhubaneswar, Odisha, India
S. Bahinipati[40], C. Kar, D. Maity[41], P. Mal, K. Naskar[41], A. Nayak[41], S. Nayak, K. Pal, P. Sadangi, S.K. Swain, S. Varghese[41], D. Vats[41]

Indian Institute of Science Education and Research (IISER), Pune, India
S. Acharya[42], A. Alpana, S. Dube, B. Gomber[42], P. Hazarika, B. Kansal, A. Laha, B. Sahu[42], S. Sharma, K.Y. Vaish

Isfahan University of Technology, Isfahan, Iran
H. Bakhshiansohi[43], A. Jafari[44], M. Zeinali[45]

Institute for Research in Fundamental Sciences (IPM), Tehran, Iran
S. Bashiri, S. Chenarani[46], S.M. Etesami, Y. Hosseini, M. Khakzad, E. Khazaie, M. Mohammadi Najafabadi, S. Tizchang[47]

University College Dublin, Dublin, Ireland
M. Felcini, M. Grunewald

INFN Sezione di Bari[a], Università di Bari[b], Politecnico di Bari[c], Bari, Italy
M. Abbrescia[a,b], A. Colaleo[a,b], D. Creanza[a,c], B. D'Anzi[a,b], N. De Filippis[a,c], M. De Palma[a,b], W. Elmetenawee[a,b,17], N. Ferrara[a,b], L. Fiore[a], G. Iaselli[a,c], L. Longo[a], M. Louka[a,b], G. Maggi[a,c], M. Maggi[a], I. Margjeka[a], V. Mastrapasqua[a,b], S. My[a,b], S. Nuzzo[a,b], A. Pellecchia[a,b], A. Pompili[a,b], G. Pugliese[a,c], R. Radogna[a,b], D. Ramos[a], A. Ranieri[a], L. Silvestris[a], F.M. Simone[a,c], Ü. Sözbilir[a], A. Stamerra[a,b], D. Troiano[a,b], R. Venditti[a,b], P. Verwilligen[a], A. Zaza[a,b]

INFN Sezione di Bologna[a], Università di Bologna[b], Bologna, Italy
G. Abbiendi[a], C. Battilana[a,b], D. Bonacorsi[a,b], P. Capiluppi[a,b], A. Castro[†a,b], F.R. Cavallo[a], M. Cuffiani[a,b], G.M. Dallavalle[a], T. Diotalevi[a,b], F. Fabbri[a], A. Fanfani[a,b], D. Fasanella[a], P. Giacomelli[a], L. Giommi[a,b], C. Grandi[a], L. Guiducci[a,b], S. Lo Meo[a,48], M. Lorusso[a,b], L. Lunerti[a], S. Marcellini[a], G. Masetti[a], F.L. Navarria[a,b], G. Paggi[a,b], A. Perrotta[a], F. Primavera[a,b], A.M. Rossi[a,b], S. Rossi Tisbeni[a,b], T. Rovelli[a,b], G.P. Siroli[a,b]

INFN Sezione di Catania[a], Università di Catania[b], Catania, Italy
S. Costa[a,b,49], A. Di Mattia[a], A. Lapertosa[a], R. Potenza[a,b], A. Tricomi[a,b,49]

INFN Sezione di Firenze[a], Università di Firenze[b], Firenze, Italy

P. Assiouras[a], G. Barbagli[a], G. Bardelli[a,b], M. Bartolini[a,b], B. Camaiani[a,b], A. Cassese[a], R. Ceccarelli[a], V. Ciulli[a,b], C. Civinini[a], R. D'Alessandro[a,b], E. Focardi[a,b], T. Kello[a], G. Latino[a,b], P. Lenzi[a,b], M. Lizzo[a], M. Meschini[a], S. Paoletti[a], A. Papanastassiou[a,b], G. Sguazzoni[a], L. Viliani[a]

INFN Laboratori Nazionali di Frascati, Frascati, Italy
L. Benussi, S. Bianco, S. Meola[50], D. Piccolo

INFN Sezione di Genova[a], Università di Genova[b], Genova, Italy
M. Alves Gallo Pereira[a], F. Ferro[a], E. Robutti[a], S. Tosi[a,b]

INFN Sezione di Milano-Bicocca[a], Università di Milano-Bicocca[b], Milano, Italy
A. Benaglia[a], F. Brivio[a], F. Cetorelli[a,b], F. De Guio[a,b], M.E. Dinardo[a,b], P. Dini[a], S. Gennai[a], R. Gerosa[a,b], A. Ghezzi[a,b], P. Govoni[a,b], L. Guzzi[a], G. Lavizzari[a,b], M.T. Lucchini[a,b], M. Malberti[a], S. Malvezzi[a], A. Massironi[a], D. Menasce[a], L. Moroni[a], M. Paganoni[a,b], S. Palluotto[a,b], D. Pedrini[a], A. Perego[a,b], B.S. Pinolini[a], G. Pizzati[a,b], S. Ragazzi[a,b], T. Tabarelli de Fatis[a,b]

INFN Sezione di Napoli[a], Università di Napoli 'Federico II'[b], Napoli, Italy; Università della Basilicata[c], Potenza, Italy; Scuola Superiore Meridionale (SSM)[d], Napoli, Italy
S. Buontempo[a], A. Cagnotta[a,b], F. Carnevali[a,b], N. Cavallo[a,c], F. Fabozzi[a,c], A.O.M. Iorio[a,b], L. Lista[a,b,51], P. Paolucci[a,29], B. Rossi[a]

INFN Sezione di Padova[a], Università di Padova[b], Padova, Italy; Universita degli Studi di Cagliari[c], Cagliari, Italy
R. Ardino[a], P. Azzi[a], N. Bacchetta[a,52], P. Bortignon[a], G. Bortolato[a,b], A.C.M. Bulla[a], R. Carlin[a,b], T. Dorigo[a,53], F. Fanzago[a], F. Gasparini[a,b], U. Gasparini[a,b], S. Giorgetti[a], F. Gonella[a], E. Lusiani[a], M. Margoni[a,b], A.T. Meneguzzo[a,b], M. Migliorini[a,b], J. Pazzini[a,b], P. Ronchese[a,b], R. Rossin[a,b], F. Simonetto[a,b], M. Tosi[a,b], A. Triossi[a,b], S. Ventura[a], M. Zanetti[a,b], P. Zotto[a,b], A. Zucchetta[a,b], G. Zumerle[a,b]

INFN Sezione di Pavia[a], Università di Pavia[b], Pavia, Italy
A. Braghieri[a], S. Calzaferri[a], D. Fiorina[a], P. Montagna[a,b], V. Re[a], C. Riccardi[a,b], P. Salvini[a], I. Vai[a,b], P. Vitulo[a,b]

INFN Sezione di Perugia[a], Università di Perugia[b], Perugia, Italy
S. Ajmal[a,b], M.E. Ascioti[a,b], G.M. Bilei[a], C. Carrivale[a,b], D. Ciangottini[a,b], L. Fanò[a,b], V. Mariani[a,b], M. Menichelli[a], F. Moscatelli[a,54], A. Rossi[a,b], A. Santocchia[a,b], D. Spiga[a], T. Tedeschi[a,b]

INFN Sezione di Pisa[a], Università di Pisa[b], Scuola Normale Superiore di Pisa[c], Pisa, Italy; Università di Siena[d], Siena, Italy
C. Aimè[a], C.A. Alexe[a,c], P. Asenov[a,b], P. Azzurri[a], G. Bagliesi[a], R. Bhattacharya[a], L. Bianchini[a,b], T. Boccali[a], E. Bossini[a], D. Bruschini[a,c], R. Castaldi[a], M.A. Ciocci[a,b], M. Cipriani[a,b], V. D'Amante[a,d], R. Dell'Orso[a], S. Donato[a,b], A. Giassi[a], F. Ligabue[a,c], A.C. Marini[a,b], D. Matos Figueiredo[a], A. Messineo[a,b], S. Mishra[a], V.K. Muraleedharan Nair Bindhu[a,b,41], M. Musich[a,b], S. Nandan[a], F. Palla[a], A. Rizzi[a,b], G. Rolandi[a,c], S. Roy Chowdhury[a], T. Sarkar[a], A. Scribano[a], P. Spagnolo[a], F. Tenchini[a,b], R. Tenchini[a], G. Tonelli[a,b], N. Turini[a,d], F. Vaselli[a,c], A. Venturi[a], P.G. Verdini[a]

INFN Sezione di Roma[a], Sapienza Università di Roma[b], Roma, Italy
P. Barria[a], C. Basile[a,b], F. Cavallari[a], L. Cunqueiro Mendez[a,b], D. Del Re[a,b],

E. Di Marco[a,b], M. Diemoz[a], F. Errico[a,b], R. Gargiulo[a,b], E. Longo[a,b], L. Martikainen[a,b], J. Mijuskovic[a,b], G. Organtini[a,b], F. Pandolfi[a], R. Paramatti[a,b], C. Quaranta[a,b], S. Rahatlou[a,b], C. Rovelli[a], F. Santanastasio[a,b], L. Soffi[a], V. Vladimirov[a,b]

INFN Sezione di Torino[a], Università di Torino[b], Torino, Italy; Università del Piemonte Orientale[c], Novara, Italy
N. Amapane[a,b], R. Arcidiacono[a,c], S. Argiro[a,b], M. Arneodo[a,c], N. Bartosik[a], R. Bellan[a,b], C. Biino[a], C. Borca[a,b], N. Cartiglia[a], M. Costa[a,b], R. Covarelli[a,b], N. Demaria[a], L. Finco[a], M. Grippo[a,b], B. Kiani[a,b], F. Legger[a], F. Luongo[a,b], C. Mariotti[a], L. Markovic[a,b], S. Maselli[a], A. Mecca[a,b], L. Menzio[a,b], P. Meridiani[a], E. Migliore[a,b], M. Monteno[a], R. Mulargia[a], M.M. Obertino[a,b], G. Ortona[a], L. Pacher[a,b], N. Pastrone[a], M. Pelliccioni[a], M. Ruspa[a,c], F. Siviero[a,b], V. Sola[a,b], A. Solano[a,b], A. Staiano[a], C. Tarricone[a,b], D. Trocino[a], G. Umoret[a,b], R. White[a,b]

INFN Sezione di Trieste[a], Università di Trieste[b], Trieste, Italy
J. Babbar[a,b], S. Belforte[a], V. Candelise[a,b], M. Casarsa[a], F. Cossutti[a], K. De Leo[a], G. Della Ricca[a,b]

Kyungpook National University, Daegu, Korea
S. Dogra, J. Hong, J. Kim, D. Lee, H. Lee, S.W. Lee, C.S. Moon, Y.D. Oh, M.S. Ryu, S. Sekmen, B. Tae, Y.C. Yang

Department of Mathematics and Physics - GWNU, Gangneung, Korea
M.S. Kim

Chonnam National University, Institute for Universe and Elementary Particles, Kwangju, Korea
G. Bak, P. Gwak, H. Kim, D.H. Moon

Hanyang University, Seoul, Korea
E. Asilar, J. Choi[55], D. Kim, T.J. Kim, J.A. Merlin, Y. Ryou

Korea University, Seoul, Korea
S. Choi, S. Han, B. Hong, K. Lee, K.S. Lee, S. Lee, J. Yoo

Kyung Hee University, Department of Physics, Seoul, Korea
J. Goh, S. Yang

Sejong University, Seoul, Korea
Y. Kang, H. S. Kim, Y. Kim, S. Lee

Seoul National University, Seoul, Korea
J. Almond, J.H. Bhyun, J. Choi, J. Choi, W. Jun, J. Kim, Y.W. Kim, S. Ko, H. Lee, J. Lee, J. Lee, B.H. Oh, S.B. Oh, H. Seo, U.K. Yang, I. Yoon

University of Seoul, Seoul, Korea
W. Jang, D.Y. Kang, S. Kim, B. Ko, J.S.H. Lee, Y. Lee, I.C. Park, Y. Roh, I.J. Watson

Yonsei University, Department of Physics, Seoul, Korea
S. Ha, K. Hwang, B. Kim, K. Lee, H.D. Yoo

Sungkyunkwan University, Suwon, Korea
M. Choi, M.R. Kim, H. Lee, Y. Lee, I. Yu

College of Engineering and Technology, American University of the Middle East (AUM),

Dasman, Kuwait
T. Beyrouthy, Y. Gharbia

Kuwait University - College of Science - Department of Physics, Safat, Kuwait
F. Alazemi

Riga Technical University, Riga, Latvia
K. Dreimanis, A. Gaile, C. Munoz Diaz, D. Osite, G. Pikurs, A. Potrebko, M. Seidel, D. Sidiropoulos Kontos

University of Latvia (LU), Riga, Latvia
N.R. Strautnieks

Vilnius University, Vilnius, Lithuania
M. Ambrozas, A. Juodagalvis, A. Rinkevicius, G. Tamulaitis

National Centre for Particle Physics, Universiti Malaya, Kuala Lumpur, Malaysia
I. Yusuff[56], Z. Zolkapli

Universidad de Sonora (UNISON), Hermosillo, Mexico
J.F. Benitez, A. Castaneda Hernandez, H.A. Encinas Acosta, L.G. Gallegos Maríñez, M. León Coello, J.A. Murillo Quijada, A. Sehrawat, L. Valencia Palomo

Centro de Investigacion y de Estudios Avanzados del IPN, Mexico City, Mexico
G. Ayala, H. Castilla-Valdez, H. Crotte Ledesma, E. De La Cruz-Burelo, I. Heredia-De La Cruz[57], R. Lopez-Fernandez, J. Mejia Guisao, A. Sánchez Hernández

Universidad Iberoamericana, Mexico City, Mexico
C. Oropeza Barrera, D.L. Ramirez Guadarrama, M. Ramírez García

Benemerita Universidad Autonoma de Puebla, Puebla, Mexico
I. Bautista, F.E. Neri Huerta, I. Pedraza, H.A. Salazar Ibarguen, C. Uribe Estrada

University of Montenegro, Podgorica, Montenegro
I. Bubanja, N. Raicevic

University of Canterbury, Christchurch, New Zealand
P.H. Butler

National Centre for Physics, Quaid-I-Azam University, Islamabad, Pakistan
A. Ahmad, M.I. Asghar, A. Awais, M.I.M. Awan, H.R. Hoorani, W.A. Khan

AGH University of Krakow, Krakow, Poland
V. Avati, A. Bellora, L. Forthomme, L. Grzanka, M. Malawski, K. Piotrzkowski

National Centre for Nuclear Research, Swierk, Poland
H. Bialkowska, M. Bluj, M. Górski, M. Kazana, M. Szleper, P. Zalewski

Institute of Experimental Physics, Faculty of Physics, University of Warsaw, Warsaw, Poland
K. Bunkowski, K. Doroba, A. Kalinowski, M. Konecki, J. Krolikowski, A. Muhammad

Warsaw University of Technology, Warsaw, Poland
P. Fokow, K. Pozniak, W. Zabolotny

Laboratório de Instrumentação e Física Experimental de Partículas, Lisboa, Portugal
M. Araujo, D. Bastos, C. Beirão Da Cruz E Silva, A. Boletti, M. Bozzo, T. Camporesi, G. Da Molin, P. Faccioli, M. Gallinaro, J. Hollar, N. Leonardo,

G.B. Marozzo, A. Petrilli, M. Pisano, J. Seixas, J. Varela, J.W. Wulff

Faculty of Physics, University of Belgrade, Belgrade, Serbia
P. Adzic, P. Milenovic

VINCA Institute of Nuclear Sciences, University of Belgrade, Belgrade, Serbia
D. Devetak, M. Dordevic, J. Milosevic, L. Nadderd, V. Rekovic, M. Stojanovic

Centro de Investigaciones Energéticas Medioambientales y Tecnológicas (CIEMAT), Madrid, Spain
J. Alcaraz Maestre, Cristina F. Bedoya, J.A. Brochero Cifuentes, Oliver M. Carretero, M. Cepeda, M. Cerrada, N. Colino, B. De La Cruz, A. Delgado Peris, A. Escalante Del Valle, D. Fernández Del Val, J.P. Fernández Ramos, J. Flix, M.C. Fouz, O. Gonzalez Lopez, S. Goy Lopez, J.M. Hernandez, M.I. Josa, J. Llorente Merino, C. Martin Perez, E. Martin Viscasillas, D. Moran, C. M. Morcillo Perez, Á. Navarro Tobar, C. Perez Dengra, A. Pérez-Calero Yzquierdo, J. Puerta Pelayo, I. Redondo, J. Sastre, J. Vazquez Escobar

Universidad Autónoma de Madrid, Madrid, Spain
J.F. de Trocóniz

Universidad de Oviedo, Instituto Universitario de Ciencias y Tecnologías Espaciales de Asturias (ICTEA), Oviedo, Spain
B. Alvarez Gonzalez, J. Cuevas, J. Fernandez Menendez, S. Folgueras, I. Gonzalez Caballero, P. Leguina, E. Palencia Cortezon, J. Prado Pico, V. Rodríguez Bouza, A. Soto Rodríguez, A. Trapote, C. Vico Villalba, P. Vischia

Instituto de Física de Cantabria (IFCA), CSIC-Universidad de Cantabria, Santander, Spain
S. Blanco Fernández, I.J. Cabrillo, A. Calderon, J. Duarte Campderros, M. Fernandez, G. Gomez, C. Lasaosa García, R. Lopez Ruiz, C. Martinez Rivero, P. Martinez Ruiz del Arbol, F. Matorras, P. Matorras Cuevas, E. Navarrete Ramos, J. Piedra Gomez, L. Scodellaro, I. Vila, J.M. Vizan Garcia

University of Colombo, Colombo, Sri Lanka
B. Kailasapathy[58], D.D.C. Wickramarathna

University of Ruhuna, Department of Physics, Matara, Sri Lanka
W.G.D. Dharmaratna[59], K. Liyanage, N. Perera

CERN, European Organization for Nuclear Research, Geneva, Switzerland
D. Abbaneo, C. Amendola, E. Auffray, J. Baechler, D. Barney, A. Bermúdez Martínez, M. Bianco, A.A. Bin Anuar, A. Bocci, L. Borgonovi, C. Botta, A. Bragagnolo, E. Brondolin, C.E. Brown, C. Caillol, G. Cerminara, N. Chernyavskaya, D. d'Enterria, A. Dabrowski, A. David, A. De Roeck, M.M. Defranchis, M. Deile, M. Dobson, G. Franzoni, W. Funk, S. Giani, D. Gigi, K. Gill, F. Glege, M. Glowacki, J. Hegeman, J.K. Heikkilä, B. Huber, V. Innocente, T. James, P. Janot, O. Kaluzinska, O. Karacheban[27], G. Karathanasis, S. Laurila, P. Lecoq, E. Leutgeb, C. Lourenço, M. Magherini, L. Malgeri, M. Mannelli, M. Matthewman, A. Mehta, F. Meijers, S. Mersi, E. Meschi, V. Milosevic, F. Monti, F. Moortgat, M. Mulders, I. Neutelings, S. Orfanelli, F. Pantaleo, G. Petrucciani, A. Pfeiffer, M. Pierini, M. Pitt, H. Qu, D. Rabady, B. Ribeiro Lopes, F. Riti, M. Rovere, H. Sakulin, R. Salvatico, S. Sanchez Cruz, S. Scarfi, M. Selvaggi, A. Sharma, K. Shchelina, P. Silva, P. Sphicas[60], A.G. Stahl Leiton, A. Steen, S. Summers, D. Treille, P. Tropea, D. Walter,

J. Wanczyk[61], J. Wang, S. Wuchterl, P. Zehetner, P. Zejdl, W.D. Zeuner

PSI Center for Neutron and Muon Sciences, Villigen, Switzerland
T. Bevilacqua[62], L. Caminada[62], A. Ebrahimi, W. Erdmann, R. Horisberger, Q. Ingram, H.C. Kaestli, D. Kotlinski, C. Lange, M. Missiroli[62], L. Noehte[62], T. Rohe, A. Samalan

ETH Zurich - Institute for Particle Physics and Astrophysics (IPA), Zurich, Switzerland
T.K. Aarrestad, M. Backhaus, G. Bonomelli, A. Calandri, C. Cazzaniga, K. Datta, P. De Bryas Dexmiers D'archiac[61], A. De Cosa, G. Dissertori, M. Dittmar, M. Donegà, F. Eble, M. Galli, K. Gedia, F. Glessgen, C. Grab, N. Härringer, T.G. Harte, D. Hits, W. Lustermann, A.-M. Lyon, R.A. Manzoni, M. Marchegiani, L. Marchese, A. Mascellani[61], F. Nessi-Tedaldi, F. Pauss, V. Perovic, S. Pigazzini, B. Ristic, R. Seidita, J. Steggemann[61], A. Tarabini, D. Valsecchi, R. Wallny

Universität Zürich, Zurich, Switzerland
C. Amsler[63], P. Bärtschi, M.F. Canelli, K. Cormier, M. Huwiler, W. Jin, A. Jofrehei, B. Kilminster, S. Leontsinis, S.P. Liechti, A. Macchiolo, P. Meiring, F. Meng, J. Motta, A. Reimers, P. Robmann, M. Senger, E. Shokr, F. Stäger, R. Tramontano

National Central University, Chung-Li, Taiwan
C. Adloff[64], D. Bhowmik, C.M. Kuo, W. Lin, P.K. Rout, P.C. Tiwari[37]

National Taiwan University (NTU), Taipei, Taiwan
L. Ceard, K.F. Chen, Z.g. Chen, A. De Iorio, W.-S. Hou, T.h. Hsu, Y.w. Kao, S. Karmakar, G. Kole, Y.y. Li, R.-S. Lu, E. Paganis, X.f. Su, J. Thomas-Wilsker, L.s. Tsai, D. Tsionou, H.y. Wu, E. Yazgan

High Energy Physics Research Unit, Department of Physics, Faculty of Science, Chulalongkorn University, Bangkok, Thailand
C. Asawatangtrakuldee, N. Srimanobhas, V. Wachirapusitanand

Tunis El Manar University, Tunis, Tunisia
Y. Maghrbi

Çukurova University, Physics Department, Science and Art Faculty, Adana, Turkey
D. Agyel, F. Boran, F. Dolek, I. Dumanoglu[65], E. Eskut, Y. Guler[66], E. Gurpinar Guler[66], C. Isik, O. Kara, A. Kayis Topaksu, Y. Komurcu, G. Onengut, K. Ozdemir[67], A. Polatoz, B. Tali[68], U.G. Tok, E. Uslan, I.S. Zorbakir

Middle East Technical University, Physics Department, Ankara, Turkey
M. Yalvac[69]

Bogazici University, Istanbul, Turkey
B. Akgun, I.O. Atakisi, E. Gülmez, M. Kaya[70], O. Kaya[71], S. Tekten[72]

Istanbul Technical University, Istanbul, Turkey
A. Cakir, K. Cankocak[65,73], S. Sen[74]

Istanbul University, Istanbul, Turkey
O. Aydilek[75], B. Hacisahinoglu, I. Hos[76], B. Kaynak, S. Ozkorucuklu, O. Potok, H. Sert, C. Simsek, C. Zorbilmez

Yildiz Technical University, Istanbul, Turkey

S. Cerci, B. Isildak[77], D. Sunar Cerci, T. Yetkin

Institute for Scintillation Materials of National Academy of Science of Ukraine, Kharkiv, Ukraine
A. Boyaryntsev, B. Grynyov

National Science Centre, Kharkiv Institute of Physics and Technology, Kharkiv, Ukraine
L. Levchuk

University of Bristol, Bristol, United Kingdom
D. Anthony, J.J. Brooke, A. Bundock, F. Bury, E. Clement, D. Cussans, H. Flacher, J. Goldstein, H.F. Heath, M.-L. Holmberg, L. Kreczko, S. Paramesvaran, L. Robertshaw, V.J. Smith, K. Walkingshaw Pass

Rutherford Appleton Laboratory, Didcot, United Kingdom
A.H. Ball, K.W. Bell, A. Belyaev[78], C. Brew, R.M. Brown, D.J.A. Cockerill, C. Cooke, A. Elliot, K.V. Ellis, K. Harder, S. Harper, J. Linacre, K. Manolopoulos, D.M. Newbold, E. Olaiya, D. Petyt, T. Reis, A.R. Sahasransu, G. Salvi, T. Schuh, C.H. Shepherd-Themistocleous, I.R. Tomalin, K.C. Whalen, T. Williams

Imperial College, London, United Kingdom
I. Andreou, R. Bainbridge, P. Bloch, O. Buchmuller, C.A. Carrillo Montoya, G.S. Chahal[79], D. Colling, J.S. Dancu, I. Das, P. Dauncey, G. Davies, M. Della Negra, S. Fayer, G. Fedi, G. Hall, A. Howard, G. Iles, C.R. Knight, P. Krueper, J. Langford, K.H. Law, J. León Holgado, L. Lyons, A.-M. Magnan, B. Maier, S. Mallios, M. Mieskolainen, J. Nash[80], M. Pesaresi, P.B. Pradeep, B.C. Radburn-Smith, A. Richards, A. Rose, K. Savva, C. Seez, R. Shukla, A. Tapper, K. Uchida, G.P. Uttley, T. Virdee[29], M. Vojinovic, N. Wardle, D. Winterbottom

Brunel University, Uxbridge, United Kingdom
J.E. Cole, A. Khan, P. Kyberd, I.D. Reid

Baylor University, Waco, Texas, USA
S. Abdullin, A. Brinkerhoff, E. Collins, M.R. Darwish, J. Dittmann, K. Hatakeyama, V. Hegde, J. Hiltbrand, B. McMaster, J. Samudio, S. Sawant, C. Sutantawibul, J. Wilson

Catholic University of America, Washington, DC, USA
R. Bartek, A. Dominguez, A.E. Simsek, S.S. Yu

The University of Alabama, Tuscaloosa, Alabama, USA
B. Bam, A. Buchot Perraguin, R. Chudasama, S.I. Cooper, C. Crovella, S.V. Gleyzer, E. Pearson, C.U. Perez, P. Rumerio[81], E. Usai, R. Yi

Boston University, Boston, Massachusetts, USA
A. Akpinar, C. Cosby, G. De Castro, Z. Demiragli, C. Erice, C. Fangmeier, C. Fernandez Madrazo, E. Fontanesi, D. Gastler, F. Golf, S. Jeon, J. O'cain, I. Reed, J. Rohlf, K. Salyer, D. Sperka, D. Spitzbart, I. Suarez, A. Tsatsos, A.G. Zecchinelli

Brown University, Providence, Rhode Island, USA
G. Barone, G. Benelli, D. Cutts, S. Ellis, L. Gouskos, M. Hadley, U. Heintz, K.W. Ho, J.M. Hogan[82], T. Kwon, G. Landsberg, K.T. Lau, J. Luo, S. Mondal, T. Russell, S. Sagir[83], X. Shen, M. Stamenkovic, N. Venkatasubramanian

University of California, Davis, Davis, California, USA
S. Abbott, B. Barton, C. Brainerd, R. Breedon, H. Cai, M. Calderon De La Barca Sanchez, M. Chertok, M. Citron, J. Conway, P.T. Cox, R. Erbacher, F. Jensen, O. Kukral, G. Mocellin, M. Mulhearn, S. Ostrom, W. Wei, S. Yoo, F. Zhang

University of California, Los Angeles, California, USA
K. Adamidis, M. Bachtis, D. Campos, R. Cousins, A. Datta, G. Flores Avila, J. Hauser, M. Ignatenko, M.A. Iqbal, T. Lam, Y.f. Lo, E. Manca, A. Nunez Del Prado, D. Saltzberg, V. Valuev

University of California, Riverside, Riverside, California, USA
R. Clare, J.W. Gary, G. Hanson

University of California, San Diego, La Jolla, California, USA
A. Aportela, A. Arora, J.G. Branson, S. Cittolin, S. Cooperstein, D. Diaz, J. Duarte, L. Giannini, Y. Gu, J. Guiang, R. Kansal, V. Krutelyov, R. Lee, J. Letts, M. Masciovecchio, F. Mokhtar, S. Mukherjee, M. Pieri, D. Primosch, M. Quinnan, V. Sharma, M. Tadel, E. Vourliotis, F. Würthwein, Y. Xiang, A. Yagil

University of California, Santa Barbara - Department of Physics, Santa Barbara, California, USA
A. Barzdukas, L. Brennan, C. Campagnari, K. Downham, C. Grieco, M.M. Hussain, J. Incandela, J. Kim, A.J. Li, P. Masterson, H. Mei, J. Richman, S.N. Santpur, U. Sarica, R. Schmitz, F. Setti, J. Sheplock, D. Stuart, T.Á. Vámi, X. Yan, D. Zhang

California Institute of Technology, Pasadena, California, USA
S. Bhattacharya, A. Bornheim, O. Cerri, J. Mao, H.B. Newman, G. Reales Gutiérrez, M. Spiropulu, J.R. Vlimant, C. Wang, S. Xie, R.Y. Zhu

Carnegie Mellon University, Pittsburgh, Pennsylvania, USA
J. Alison, S. An, P. Bryant, M. Cremonesi, V. Dutta, T. Ferguson, T.A. Gómez Espinosa, A. Harilal, A. Kallil Tharayil, M. Kanemura, C. Liu, T. Mudholkar, S. Murthy, P. Palit, K. Park, M. Paulini, A. Roberts, A. Sanchez, W. Terrill

University of Colorado Boulder, Boulder, Colorado, USA
J.P. Cumalat, W.T. Ford, A. Hart, A. Hassani, N. Manganelli, J. Pearkes, C. Savard, N. Schonbeck, K. Stenson, K.A. Ulmer, S.R. Wagner, N. Zipper, D. Zuolo

Cornell University, Ithaca, New York, USA
J. Alexander, X. Chen, D.J. Cranshaw, J. Dickinson, J. Fan, X. Fan, S. Hogan, P. Kotamnives, J. Monroy, M. Oshiro, J.R. Patterson, M. Reid, A. Ryd, J. Thom, P. Wittich, R. Zou

Fermi National Accelerator Laboratory, Batavia, Illinois, USA
M. Albrow, M. Alyari, O. Amram, G. Apollinari, A. Apresyan, L.A.T. Bauerdick, D. Berry, J. Berryhill, P.C. Bhat, K. Burkett, J.N. Butler, A. Canepa, G.B. Cerati, H.W.K. Cheung, F. Chlebana, G. Cummings, I. Dutta, V.D. Elvira, J. Freeman, A. Gandrakota, Z. Gecse, L. Gray, D. Green, A. Grummer, S. Grünendahl, D. Guerrero, O. Gutsche, R.M. Harris, T.C. Herwig, J. Hirschauer, B. Jayatilaka, S. Jindariani, M. Johnson, U. Joshi, T. Klijnsma, B. Klima, K.H.M. Kwok,

S. Lammel, C. Lee, D. Lincoln, R. Lipton, T. Liu, K. Maeshima, D. Mason, P. McBride, P. Merkel, S. Mrenna, S. Nahn, J. Ngadiuba, D. Noonan, S. Norberg, V. Papadimitriou, N. Pastika, K. Pedro, C. Pena[84], F. Ravera, A. Reinsvold Hall[85], L. Ristori, M. Safdari, E. Sexton-Kennedy, N. Smith, A. Soha, L. Spiegel, S. Stoynev, J. Strait, L. Taylor, S. Tkaczyk, N.V. Tran, L. Uplegger, E.W. Vaandering, I. Zoi

University of Florida, Gainesville, Florida, USA
C. Aruta, P. Avery, D. Bourilkov, P. Chang, V. Cherepanov, R.D. Field, C. Huh, E. Koenig, M. Kolosova, J. Konigsberg, A. Korytov, K. Matchev, N. Menendez, G. Mitselmakher, K. Mohrman, A. Muthirakalayil Madhu, N. Rawal, S. Rosenzweig, Y. Takahashi, J. Wang

Florida State University, Tallahassee, Florida, USA
T. Adams, A. Al Kadhim, A. Askew, S. Bower, R. Hashmi, R.S. Kim, S. Kim, T. Kolberg, G. Martinez, H. Prosper, P.R. Prova, M. Wulansatiti, R. Yohay, J. Zhang

Florida Institute of Technology, Melbourne, Florida, USA
B. Alsufyani, S. Butalla, S. Das, T. Elkafrawy[86], M. Hohlmann, E. Yanes

University of Illinois Chicago, Chicago, Illinois, USA
M.R. Adams, A. Baty, C. Bennett, R. Cavanaugh, R. Escobar Franco, O. Evdokimov, C.E. Gerber, H. Gupta, M. Hawksworth, A. Hingrajiya, D.J. Hofman, J.h. Lee, D. S. Lemos, C. Mills, S. Nanda, G. Oh, B. Ozek, D. Pilipovic, R. Pradhan, E. Prifti, P. Roy, T. Roy, S. Rudrabhatla, N. Singh, M.B. Tonjes, N. Varelas, M.A. Wadud, Z. Ye, J. Yoo

The University of Iowa, Iowa City, Iowa, USA
M. Alhusseini, D. Blend, K. Dilsiz[87], L. Emediato, G. Karaman, O.K. Köseyan, J.-P. Merlo, A. Mestvirishvili[88], O. Neogi, H. Ogul[89], Y. Onel, A. Penzo, C. Snyder, E. Tiras[90]

Johns Hopkins University, Baltimore, Maryland, USA
B. Blumenfeld, L. Corcodilos, J. Davis, A.V. Gritsan, L. Kang, S. Kyriacou, P. Maksimovic, M. Roguljic, J. Roskes, S. Sekhar, M. Swartz

The University of Kansas, Lawrence, Kansas, USA
A. Abreu, L.F. Alcerro Alcerro, J. Anguiano, S. Arteaga Escatel, P. Baringer, A. Bean, Z. Flowers, D. Grove, J. King, G. Krintiras, M. Lazarovits, C. Le Mahieu, J. Marquez, M. Murray, M. Nickel, S. Popescu[91], C. Rogan, C. Royon, S. Sanders, C. Smith, G. Wilson

Kansas State University, Manhattan, Kansas, USA
B. Allmond, R. Gujju Gurunadha, A. Ivanov, K. Kaadze, Y. Maravin, J. Natoli, D. Roy, G. Sorrentino

University of Maryland, College Park, Maryland, USA
A. Baden, A. Belloni, J. Bistany-riebman, Y.M. Chen, S.C. Eno, N.J. Hadley, S. Jabeen, R.G. Kellogg, T. Koeth, B. Kronheim, S. Lascio, A.C. Mignerey, S. Nabili, C. Palmer, C. Papageorgakis, M.M. Paranjpe, E. Popova[92], A. Shevelev, L. Wang, L. Zhang

Massachusetts Institute of Technology, Cambridge, Massachusetts, USA
C. Baldenegro Barrera, J. Bendavid, S. Bright-Thonney, I.A. Cali, P.c. Chou,

M. D'Alfonso, J. Eysermans, C. Freer, G. Gomez-Ceballos, M. Goncharov, G. Grosso, P. Harris, D. Hoang, D. Kovalskyi, J. Krupa, L. Lavezzo, Y.-J. Lee, K. Long, C. Mcginn, A. Novak, M.I. Park, C. Paus, C. Reissel, C. Roland, G. Roland, S. Rothman, G.S.F. Stephans, Z. Wang, B. Wyslouch, T. J. Yang

University of Minnesota, Minneapolis, Minnesota, USA
B. Crossman, C. Kapsiak, M. Krohn, D. Mahon, J. Mans, B. Marzocchi, M. Revering, R. Rusack, R. Saradhy, N. Strobbe

University of Nebraska-Lincoln, Lincoln, Nebraska, USA
K. Bloom, D.R. Claes, G. Haza, J. Hossain, C. Joo, I. Kravchenko, A. Rohilla, J.E. Siado, W. Tabb, A. Vagnerini, A. Wightman, F. Yan, D. Yu

State University of New York at Buffalo, Buffalo, New York, USA
H. Bandyopadhyay, L. Hay, H.w. Hsia, I. Iashvili, A. Kalogeropoulos, A. Kharchilava, M. Morris, D. Nguyen, S. Rappoccio, H. Rejeb Sfar, A. Williams, P. Young

Northeastern University, Boston, Massachusetts, USA
G. Alverson, E. Barberis, J. Bonilla, B. Bylsma, M. Campana, J. Dervan, Y. Haddad, Y. Han, I. Israr, A. Krishna, P. Levchenko, J. Li, M. Lu, R. Mccarthy, D.M. Morse, T. Orimoto, A. Parker, L. Skinnari, E. Tsai, D. Wood

Northwestern University, Evanston, Illinois, USA
S. Dittmer, K.A. Hahn, D. Li, Y. Liu, M. Mcginnis, Y. Miao, D.G. Monk, M.H. Schmitt, A. Taliercio, M. Velasco

University of Notre Dame, Notre Dame, Indiana, USA
G. Agarwal, R. Band, R. Bucci, S. Castells, A. Das, R. Goldouzian, M. Hildreth, K. Hurtado Anampa, T. Ivanov, C. Jessop, K. Lannon, J. Lawrence, N. Loukas, L. Lutton, J. Mariano, N. Marinelli, I. Mcalister, T. McCauley, C. Mcgrady, C. Moore, Y. Musienko[15], H. Nelson, M. Osherson, A. Piccinelli, R. Ruchti, A. Townsend, Y. Wan, M. Wayne, H. Yockey, M. Zarucki, L. Zygala

The Ohio State University, Columbus, Ohio, USA
A. Basnet, M. Carrigan, L.S. Durkin, C. Hill, M. Joyce, M. Nunez Ornelas, K. Wei, D.A. Wenzl, B.L. Winer, B. R. Yates

Princeton University, Princeton, New Jersey, USA
H. Bouchamaoui, K. Coldham, P. Das, G. Dezoort, P. Elmer, P. Fackeldey, A. Frankenthal, B. Greenberg, N. Haubrich, K. Kennedy, G. Kopp, S. Kwan, Y. Lai, D. Lange, A. Loeliger, D. Marlow, I. Ojalvo, J. Olsen, F. Simpson, D. Stickland, C. Tully, L.H. Vage

University of Puerto Rico, Mayaguez, Puerto Rico, USA
S. Malik, R. Sharma

Purdue University, West Lafayette, Indiana, USA
A.S. Bakshi, S. Chandra, R. Chawla, A. Gu, L. Gutay, M. Jones, A.W. Jung, A.M. Koshy, M. Liu, G. Negro, N. Neumeister, G. Paspalaki, S. Piperov, J.F. Schulte, A. K. Virdi, F. Wang, A. Wildridge, W. Xie, Y. Yao

Purdue University Northwest, Hammond, Indiana, USA
J. Dolen, N. Parashar, A. Pathak

Rice University, Houston, Texas, USA
D. Acosta, A. Agrawal, T. Carnahan, K.M. Ecklund, P.J. Fernández Manteca, S. Freed, P. Gardner, F.J.M. Geurts, I. Krommydas, W. Li, J. Lin, O. Miguel Colin, B.P. Padley, R. Redjimi, J. Rotter, E. Yigitbasi, Y. Zhang

University of Rochester, Rochester, New York, USA
A. Bodek, P. de Barbaro, R. Demina, J.L. Dulemba, A. Garcia-Bellido, O. Hindrichs, A. Khukhunaishvili, N. Parmar, P. Parygin[92], R. Taus

Rutgers, The State University of New Jersey, Piscataway, New Jersey, USA
B. Chiarito, J.P. Chou, S.V. Clark, D. Gadkari, Y. Gershtein, E. Halkiadakis, M. Heindl, C. Houghton, D. Jaroslawski, S. Konstantinou, I. Laflotte, A. Lath, R. Montalvo, K. Nash, J. Reichert, P. Saha, S. Salur, S. Schnetzer, S. Somalwar, R. Stone, S.A. Thayil, S. Thomas, J. Vora

University of Tennessee, Knoxville, Tennessee, USA
D. Ally, A.G. Delannoy, S. Fiorendi, S. Higginbotham, T. Holmes, A.R. Kanuganti, N. Karunarathna, L. Lee, E. Nibigira, S. Spanier

Texas A&M University, College Station, Texas, USA
D. Aebi, M. Ahmad, T. Akhter, K. Androsov[61], O. Bouhali[93], R. Eusebi, J. Gilmore, T. Huang, T. Kamon[94], H. Kim, S. Luo, R. Mueller, D. Overton, A. Safonov

Texas Tech University, Lubbock, Texas, USA
N. Akchurin, J. Damgov, Y. Feng, N. Gogate, Y. Kazhykarim, K. Lamichhane, S.W. Lee, C. Madrid, A. Mankel, T. Peltola, I. Volobouev

Vanderbilt University, Nashville, Tennessee, USA
E. Appelt, Y. Chen, S. Greene, A. Gurrola, W. Johns, R. Kunnawalkam Elayavalli, A. Melo, D. Rathjens, F. Romeo, P. Sheldon, S. Tuo, J. Velkovska, J. Viinikainen

University of Virginia, Charlottesville, Virginia, USA
B. Cardwell, H. Chung, B. Cox, J. Hakala, R. Hirosky, A. Ledovskoy, C. Mantilla, C. Neu, C. Ramón Álvarez

Wayne State University, Detroit, Michigan, USA
S. Bhattacharya, P.E. Karchin

University of Wisconsin - Madison, Madison, Wisconsin, USA
A. Aravind, S. Banerjee, K. Black, T. Bose, E. Chavez, S. Dasu, P. Everaerts, C. Galloni, H. He, M. Herndon, A. Herve, C.K. Koraka, A. Lanaro, R. Loveless, J. Madhusudanan Sreekala, A. Mallampalli, A. Mohammadi, S. Mondal, G. Parida, L. Pétré, D. Pinna, A. Savin, V. Shang, V. Sharma, W.H. Smith, D. Teague, H.F. Tsoi, W. Vetens, A. Warden

Authors affiliated with an international laboratory covered by a cooperation agreement with CERN
S. Afanasiev, V. Alexakhin, D. Budkouski, I. Golutvin[†], I. Gorbunov, V. Karjavine, O. Kodolova[95,92], V. Korenkov, A. Lanev, A. Malakhov, V. Matveev[96], A. Nikitenko[97,95], V. Palichik, V. Perelygin, M. Savina, V. Shalaev, S. Shmatov, S. Shulha, V. Smirnov, O. Teryaev, N. Voytishin, B.S. Yuldashev[†98], A. Zarubin, I. Zhizhin

Authors affiliated with an institute formerly covered by a cooperation agreement with CERN

G. Gavrilov, V. Golovtcov, Y. Ivanov, V. Kim[96], V. Murzin, V. Oreshkin, D. Sosnov, V. Sulimov, L. Uvarov, A. Vorobyev†, Yu. Andreev, A. Dermenev, S. Gninenko, N. Golubev, A. Karneyeu, D. Kirpichnikov, M. Kirsanov, N. Krasnikov, I. Tlisova, A. Toropin, T. Aushev, K. Ivanov, V. Gavrilov, N. Lychkovskaya, V. Popov, A. Zhokin, R. Chistov[96], M. Danilov[96], S. Polikarpov[96], V. Andreev, M. Azarkin, M. Kirakosyan, A. Terkulov, E. Boos, A. Demiyanov, A. Ershov, A. Gribushin, L. Khein, V. Korotkikh, S. Petrushanko, V. Savrin, A. Snigirev, I. Vardanyan, V. Blinov[96], T. Dimova[96], A. Kozyrev[96], O. Radchenko[96], Y. Skovpen[96], V. Kachanov, S. Slabospitskii, A. Uzunian, A. Babaev, V. Borshch, D. Druzhkin

†: Deceased
[1]Also at Yerevan State University, Yerevan, Armenia
[2]Also at TU Wien, Vienna, Austria
[3]Also at Ghent University, Ghent, Belgium
[4]Also at Universidade do Estado do Rio de Janeiro, Rio de Janeiro, Brazil
[5]Also at FACAMP - Faculdades de Campinas, Sao Paulo, Brazil
[6]Also at Universidade Estadual de Campinas, Campinas, Brazil
[7]Also at Federal University of Rio Grande do Sul, Porto Alegre, Brazil
[8]Also at University of Chinese Academy of Sciences, Beijing, China
[9]Also at China Center of Advanced Science and Technology, Beijing, China
[10]Also at University of Chinese Academy of Sciences, Beijing, China
[11]Also at China Spallation Neutron Source, Guangdong, China
[12]Now at Henan Normal University, Xinxiang, China
[13]Also at University of Shanghai for Science and Technology, Shanghai, China
[14]Now at The University of Iowa, Iowa City, Iowa, USA
[15]Also at an institute formerly covered by a cooperation agreement with CERN
[16]Also at Cairo University, Cairo, Egypt
[17]Also at Helwan University, Cairo, Egypt
[18]Also at Suez University, Suez, Egypt
[19]Now at British University in Egypt, Cairo, Egypt
[20]Also at Purdue University, West Lafayette, Indiana, USA
[21]Also at Université de Haute Alsace, Mulhouse, France
[22]Also at Istinye University, Istanbul, Turkey
[23]Also at The University of the State of Amazonas, Manaus, Brazil
[24]Also at University of Hamburg, Hamburg, Germany
[25]Also at RWTH Aachen University, III. Physikalisches Institut A, Aachen, Germany
[26]Also at Bergische University Wuppertal (BUW), Wuppertal, Germany
[27]Also at Brandenburg University of Technology, Cottbus, Germany
[28]Also at Forschungszentrum Jülich, Juelich, Germany
[29]Also at CERN, European Organization for Nuclear Research, Geneva, Switzerland
[30]Also at HUN-REN ATOMKI - Institute of Nuclear Research, Debrecen, Hungary
[31]Now at Universitatea Babes-Bolyai - Facultatea de Fizica, Cluj-Napoca, Romania
[32]Also at MTA-ELTE Lendület CMS Particle and Nuclear Physics Group, Eötvös Loránd University, Budapest, Hungary
[33]Also at HUN-REN Wigner Research Centre for Physics, Budapest, Hungary
[34]Also at Physics Department, Faculty of Science, Assiut University, Assiut, Egypt
[35]Also at Punjab Agricultural University, Ludhiana, India
[36]Also at University of Visva-Bharati, Santiniketan, India
[37]Also at Indian Institute of Science (IISc), Bangalore, India

[38]Also at Amity University Uttar Pradesh, Noida, India
[39]Also at UPES - University of Petroleum and Energy Studies, Dehradun, India
[40]Also at IIT Bhubaneswar, Bhubaneswar, India
[41]Also at Institute of Physics, Bhubaneswar, India
[42]Also at University of Hyderabad, Hyderabad, India
[43]Also at Deutsches Elektronen-Synchrotron, Hamburg, Germany
[44]Also at Isfahan University of Technology, Isfahan, Iran
[45]Also at Sharif University of Technology, Tehran, Iran
[46]Also at Department of Physics, University of Science and Technology of Mazandaran, Behshahr, Iran
[47]Also at Department of Physics, Faculty of Science, Arak University, ARAK, Iran
[48]Also at Italian National Agency for New Technologies, Energy and Sustainable Economic Development, Bologna, Italy
[49]Also at Centro Siciliano di Fisica Nucleare e di Struttura Della Materia, Catania, Italy
[50]Also at Università degli Studi Guglielmo Marconi, Roma, Italy
[51]Also at Scuola Superiore Meridionale, Università di Napoli 'Federico II', Napoli, Italy
[52]Also at Fermi National Accelerator Laboratory, Batavia, Illinois, USA
[53]Also at Lulea University of Technology, Lulea, Sweden
[54]Also at Consiglio Nazionale delle Ricerche - Istituto Officina dei Materiali, Perugia, Italy
[55]Also at Institut de Physique des 2 Infinis de Lyon (IP2I), Villeurbanne, France
[56]Also at Department of Applied Physics, Faculty of Science and Technology, Universiti Kebangsaan Malaysia, Bangi, Malaysia
[57]Also at Consejo Nacional de Ciencia y Tecnología, Mexico City, Mexico
[58]Also at Trincomalee Campus, Eastern University, Sri Lanka, Nilaveli, Sri Lanka
[59]Also at Saegis Campus, Nugegoda, Sri Lanka
[60]Also at National and Kapodistrian University of Athens, Athens, Greece
[61]Also at Ecole Polytechnique Fédérale Lausanne, Lausanne, Switzerland
[62]Also at Universität Zürich, Zurich, Switzerland
[63]Also at Stefan Meyer Institute for Subatomic Physics, Vienna, Austria
[64]Also at Laboratoire d'Annecy-le-Vieux de Physique des Particules, IN2P3-CNRS, Annecy-le-Vieux, France
[65]Also at Near East University, Research Center of Experimental Health Science, Mersin, Turkey
[66]Also at Konya Technical University, Konya, Turkey
[67]Also at Izmir Bakircay University, Izmir, Turkey
[68]Also at Adiyaman University, Adiyaman, Turkey
[69]Also at Bozok Universitetesi Rektörlügü, Yozgat, Turkey
[70]Also at Marmara University, Istanbul, Turkey
[71]Also at Milli Savunma University, Istanbul, Turkey
[72]Also at Kafkas University, Kars, Turkey
[73]Now at Istanbul Okan University, Istanbul, Turkey
[74]Also at Hacettepe University, Ankara, Turkey
[75]Also at Erzincan Binali Yildirim University, Erzincan, Turkey
[76]Also at Istanbul University - Cerrahpasa, Faculty of Engineering, Istanbul, Turkey
[77]Also at Yildiz Technical University, Istanbul, Turkey
[78]Also at School of Physics and Astronomy, University of Southampton, Southampton, United Kingdom
[79]Also at IPPP Durham University, Durham, United Kingdom
[80]Also at Monash University, Faculty of Science, Clayton, Australia

[81]Also at Università di Torino, Torino, Italy
[82]Also at Bethel University, St. Paul, Minnesota, USA
[83]Also at Karamanoğlu Mehmetbey University, Karaman, Turkey
[84]Also at California Institute of Technology, Pasadena, California, USA
[85]Also at United States Naval Academy, Annapolis, Maryland, USA
[86]Also at Ain Shams University, Cairo, Egypt
[87]Also at Bingol University, Bingol, Turkey
[88]Also at Georgian Technical University, Tbilisi, Georgia
[89]Also at Sinop University, Sinop, Turkey
[90]Also at Erciyes University, Kayseri, Turkey
[91]Also at Horia Hulubei National Institute of Physics and Nuclear Engineering (IFIN-HH), Bucharest, Romania
[92]Now at another institute formerly covered by a cooperation agreement with CERN
[93]Also at Texas A&M University at Qatar, Doha, Qatar
[94]Also at Kyungpook National University, Daegu, Korea
[95]Also at Yerevan Physics Institute, Yerevan, Armenia
[96]Also at another institute formerly covered by a cooperation agreement with CERN
[97]Also at Imperial College, London, United Kingdom
[98]Also at Institute of Nuclear Physics of the Uzbekistan Academy of Sciences, Tashkent, Uzbekistan